

# Latte++: Spatial-Temporal Voxel-based Test-Time Adaptation for Multi-Modal Segmentation

Haozhi Cao, Yuecong Xu, Pengyu Yin, Xingyu Ji, Shenghai Yuan, Jianfei Yang<sup>†</sup>, Lihua Xie *Fellow, IEEE*,

**Abstract**—Multi-modal test-time adaptation (MM-TTA) is proposed to adapt models to an unlabeled target domain by leveraging the complementary multi-modal inputs in an online manner. Previous MM-TTA methods for 3D segmentation rely on predictions of cross-modal information in each input frame, while they ignore the fact that predictions of geometric neighborhoods within consecutive frames are highly correlated, leading to unstable predictions across time. To fulfill this gap, we propose ReLIable Spatial-temporal Voxels (Latte), an MM-TTA method that leverages reliable cross-modal spatial-temporal correspondences for multi-modal 3D segmentation. Motivated by the fact that reliable predictions should be consistent with their spatial-temporal correspondences, Latte aggregates consecutive frames in a sliding-window manner and constructs Spatial-Temporal (ST) voxels to capture temporally local prediction consistency for each modality. After filtering out ST voxels with high ST entropy, Latte conducts cross-modal learning for each point and pixel by attending to those with reliable and consistent predictions among both spatial and temporal neighborhoods. Considering the prediction consistency might vary under different sliding windows, we further propose Latte++ which leverages ST voxels generated under various sliding windows to more thoroughly evaluate intra-modal prediction consistency before the cross-modal fusion. Experimental results show that both Latte and Latte++ achieve state-of-the-art performance on five MM-TTA benchmarks compared to previous MM-TTA or TTA methods. Code will be available at <https://github.com/AronCao49/Latte-plusplus>.

**Index Terms**—Test-time adaptation, multi-modal learning, 3D semantic segmentation

## I. INTRODUCTION

**3**D semantic segmentation [13], [23] is a fundamental task to achieve various fully autonomous applications such as autonomous driving and robot navigation [12], [16], [22]. With the increasing urge for robust sensing, multi-modal sensors (e.g., cameras and LiDARs) are widely adopted in autonomous systems, containing rich complementary information from different sensors. However, conventional deep-learning-based solutions lean on expensive point-wise annotations and perform poorly on data from different domains due to the domain

Haozhi Cao, Pengyu Yin, Xingyu Ji, Shenghai Yuan, and Lihua Xie are with Centre for Advanced Robotics Technology Innovation (CARTIN), Nanyang Technological University. Email: {haozhi002, pengyu001, xingyu001, shuyuan, elhxie}@ntu.edu.sg.

Yuecong Xu is with Department of Electrical and Computer Engineering, National University of Singapore. Email: yc.xu@nus.edu.sg.

Jianfei Yang is with School of Electrical and Electronic Engineering and School of Mechanical and Aerospace Engineering, Nanyang Technological University. Email: jianfei.yang@ntu.edu.sg.

This research is supported by the National Research Foundation, Singapore, under the NRF Medium Sized Centre scheme (CARTIN). Any opinions, findings and conclusions or recommendations expressed in this material are those of the author(s) and do not reflect the views of National Research Foundation, Singapore.

<sup>†</sup>Corresponding author.

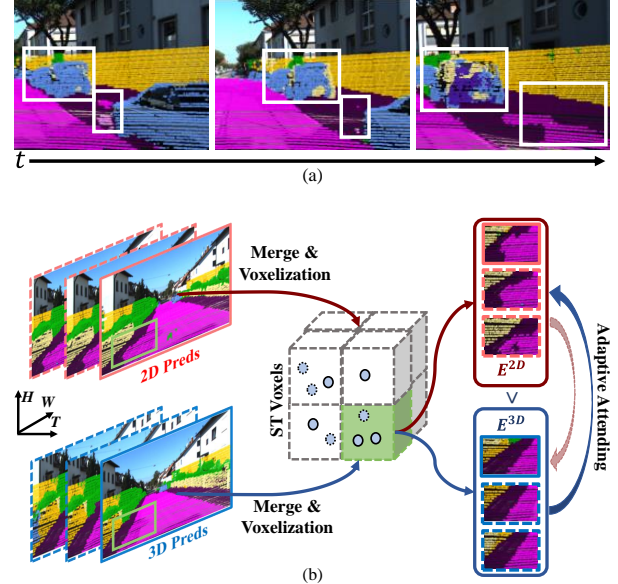


Fig. 1. Illustration of previous MM-TTA methods and our Latte. (a) visualizes the predictions from the previous state-of-the-art MM-TTA method [44] in consecutive frames on SemanticKITTI [2], where regions in white boxes exhibit noisy predictions when considering single-frame input. (b) presents the overall framework of Latte, which firstly obtains ST voxels for each modality given the merged input of consecutive frames within each sliding window and then computes the modality-specific ST entropy  $E^{2D}$ ,  $E^{3D}$ . ST entropy indicates the relative reliability of each voxel in each modality and therefore is utilized in the following adaptive cross-modal attending.

shift [11], [41], [48]. To resolve this problem, previous works have proposed Multi-Modal Unsupervised Domain Adaptation (MM-UDA) approaches [25], [29], [38], [61] that employ multi-modal information to transfer knowledge learned from the labeled source domain to the unlabeled target domain without expensive human annotations.

Nevertheless, the adaptation process of MM-UDA is completely offline, which requires full access to the source domain dataset and multiple training epochs. Despite its effectiveness, offline training is usually infeasible when encountering distribution shifts during the inference stage that demand adapting models in real-time. Inspired by Test-Time Adaptation (TTA) [36], [37], a recent work [44] proposes the first Multi-Modal Test-Time Adaptation (MM-TTA) method for 3D segmentation. Similar to the settings of TTA, MM-TTA prohibits access to any raw sample from the source domain dataset and adapts the model during the testing stage. This results in a *quick adaptation* scenario (i.e., one epoch for training only as in [44], [47]) that requires stable optimization in an online manner. To this end, MM-TTA methods must seek

a reliable source of supervision signals.

To fulfill the efficiency and stability of adaptation, the current state-of-the-art MM-TTA method [44] evaluates modal reliability by the prediction consistency between different experts in a frame-wise manner. However, due to the domain shift between the online frame and the pre-trained source dataset, the single-frame prediction is usually unstable. Existing approaches rely on pseudo labels to refine the single-frame prediction but still fail in some cases. As shown in Fig. 1a, the single-frame refinement strategy [44] suffers from noisy single-frame predictions on the car in the white rectangle across time. Such inconsistent predictions across time degenerate the segmentation performance and aggravate denoising stress in downstream tasks (*e.g.*, semantic-based retrieval [63] and obstacle recognition). On one hand, these temporally unstable single-frame predictions could be wrongly regarded as reliable ones, propagating prediction noise to the other modality and causing error accumulation or even catastrophic forgetting [36], [37]. On the other hand, while previous methods [7], [56] alleviate this instability by utilizing the average predictions of multiple augmented frames instead, they are computationally expensive for online adaptation since the inference time grows linearly with the increasing number of augmented frames.

This work aims to efficiently suppress the single-frame instability for MM-TTA by exploiting the correlation between multi-frame correspondences. Specifically, we propose that 3D space can be efficiently divided into multiple voxels [48], each of which contains points and point-corresponding pixels located at the same geometric region. While captured at different timestamps, points or pixels located at the same voxel can be viewed as different observations on the same semantic object [43]. Reliable predictions should therefore be certain and consistent within their corresponding voxels across time, whether we evaluate them from a temporally global perspective (*i.e.*, all input frames) or a temporally local perspective (*i.e.*, consecutive frames within any time window). By aggregating the predictions in a voxel-wise manner and re-evaluating their reliability, the single-frame prediction noise as in Fig. 1(a) can be effectively alleviated.

Motivated by the above observation, we propose a novel MM-TTA method called **ReLiable Spatial-temporal Voxels (Latte)**, which leverages the spatial-temporal correspondences within consecutive frames in a cross-modal manner as in Fig. 1(b). Specifically, given frames of point clouds with their estimated poses, we regard points in the same voxel extracted from the merged point cloud frames as spatial-temporal correspondences. Different from previous works that merge all input frames [9], [14] or regularize frame-to-frame consistency [43], Latte aggregates consecutive frames in a sliding-window manner to estimate the temporally local prediction consistency through the proposed Spatial-Temporal voxels (ST voxels) and entropy (ST entropy). Based on the reliability estimated by ST entropy, we conduct cross-modal learning in an adaptive attending manner to reduce the contributions of predictions from the noisy modality.

Despite the effectiveness of Latte, the resulting ST voxels greatly depend on the pre-defined window size for frame

aggregation. Different semantic classes and objects, however, are best evaluated using different sizes of time windows. For instance, dynamic objects across frames should be evaluated among smaller windows to reduce the incorrect correspondences caused by the shadow-like effect [10], while static environmental backgrounds could benefit from a larger aggregation window size to introduce more spatial-temporal correspondences. This motivates us to extend Latte as **Latte++**, which performs consistency evaluation under different aggregation windows to achieve a better reliability estimation in an intra-modal manner. Specifically, Latte++ aggregates consecutive frames within different sizes of sliding windows, resulting in window-wise ST voxels and entropy. Window-wise predictions and ST entropy are then adaptively combined based on their consistency level so that the prediction reliability of different semantic classes is better evaluated for each modality before the cross-modal fusion.

To facilitate the progress of MM-TTA, we evaluate Latte and existing TTA methods with more recent backbones (SegFormer [60] and SPVCNN [48]) across five different benchmarks under two different MM-TTA schemes (*i.e.*, a stationary target domain [44], namely MM-TTA, or a *continually* changing target domain, namely MM-CTTA [7]). Experimental results show that Latte and Latte++ consistently outperform previous TTA/MM-TTA methods on both MM-TTA and MM-CTTA schemes across five different benchmarks. Our contributions are summarized as follows:

- We propose Latte, a novel MM-TTA method for multi-modal 3D segmentation, which is the first work incorporating spatial-temporal correlations for MM-TTA segmentation to our best knowledge.
- Latte efficiently extracts spatial-temporal correspondence through ST voxels and estimates their reliability by ST entropy, which is further incorporated to enhance adaptive cross-modal attending.
- We further propose Latte++, which generates ST voxels and entropy under different aggregation schemes to better evaluate the intra-modal prediction reliability in a voxel-wise manner.
- Experimental results show that Latte outperforms previous state-of-the-art TTA or MM-TTA methods on five benchmarks under MM-TTA or MM-CTTA schemes.

This paper extends our previous work [5] in the following aspects. Instead of using a single frame aggregation strategy [5], we propose to aggregate frames with various window sizes to better evaluate the prediction reliability of different semantic classes. We also extend our literature review to cover more recent TTA methods, discussing the development of TTA methods from different trends and highlighting our contributions. Besides MM-TTA, we extend our evaluation task to Multi-Modal *Continual* Test-Time Adaptation (MM-CTTA) [7], a newly introduced and more challenging scenario with continually changing target domains rather than a stationary one as in MM-TTA. Comprehensive quantitative and qualitative comparisons, along with ablation studies, are conducted to more effectively demonstrate the advantages of Latte and Latte++ when tackling MM-TTA and MM-CTTA.

## II. RELATED WORKS

**Test-Time Adaptation (TTA).** TTA is proposed to mitigate the domain shift between the inaccessible training source domain and the testing target domain. Different from source-free adaptation [31], [45] which also discards the access to the source domain yet requires multiple training epochs, the adaptation process of TTA is completely online, following the “one-pass” protocol as in [47]. Existing TTA methods can be categorized into two types based on their adaptation strategies [30], including offline TTA methods (*e.g.*, source-free domain adaptation [8], [28], [32], [67] and test-time training) and online TTA methods<sup>1</sup>. Due to its practical and challenging setting, TTA is attracting more and more attention. Previously proposed TTA methods, which mainly target image classification, can be divided into two categories: i) backpropagation(BP)-free TTA, and ii) BP-based TTA. BP-free TTA methods consider a challenging scenario where computational resources are limited, which therefore restricts updating learnable parameters through backpropagation. They therefore propose various solutions without updating most of the network parameters, such as batch normalization adaptation [18], [66], output logit adaptation [3], and prompt adaptation using forward-pass only [35]. Despite its efficiency, the prohibition of updating parameters usually limits the adaptation capacity of BP-free TTA methods, leading to inferior performance compared to BP-based TTA methods.

BP-based TTA methods, on the other hand, attempt to address this task by proposing unsupervised online objectives from different perspectives, such as entropy minimization [36], [37], [54], self-training with pseudo-labels [20], [55], and augmentation invariance [56], [65]. In addition to regularizing predictions, some methods propose to adapt networks from the feature level instead [34], [47], while more recent methods begin to consider different variants of TTA scenarios, such as continual TTA [7], [36], [56], non-i.i.d TTA [19], or the mix of aforementioned cases [64]. While both existing BP-free and BP-based TTA methods apply to multi-modal 3D semantic segmentation, they omit the existing spatial-temporal correlations within consecutive scans and therefore are incapable of addressing inconsistency issues as in Fig. 1a. In this work, we argue temporal information in 3D segmentation can be effectively leveraged for TTA as Latte in this work.

**Multi-modal domain adaptation for 3D segmentation.** To avoid expensive annotation costs and overcome the poor generalizability of fully supervised solutions, various multi-modal domain adaptation methods have been investigated. Existing methods can be roughly divided into three types based on their adaptation settings: (i) MM-UDA, which requires full access to both source and target domains and offline training, (ii) Multi-Modal Source-Free Domain Adaptation (MM-SFDA), which relies on offline training with the target domain only, and (iii) MM-TTA, which is performed online on the target domain during the inference process. For MM-UDA, xMUDA [25] is the primary work that incorporates cross-modal learning with MM-UDA. It regards cross-modal prediction consistency and

pseudo-labels as its supervision signals in the unlabeled target domain. Most subsequent works propose solutions to address its limitations from different perspectives, such as more diverse point-pixel correspondence [38], [61], procedures to mitigate domain gaps [29], [33], and alleviating class-imbalanced problem [6]. Inspired by the recent success of the Vision Foundation Model (VFM) [1], [27] and Language-Image Pre-Training (CLIP) [42], some recent MM-UDA methods [6], [39], [57], [58] attempt to leverage VFM or CLIP as the domain invariant feature to achieve better transferring usable knowledge to the target domains. Specifically, MoPA [6] proposes to encourage consistent predictions within the filtered unlabeled semantic masks provided by SAM [27], while the following works [39], [57], [58] further extend this knowledge transferring techniques from a feature-level perspective. Specifically, UniDSeg [57] introduces additional lightweight learnable modules between layers of VFM to facilitate the transitional prompting between modalities, whereas Peng *et al.* [39] propose a simpler alternative to align the 3D features to the ones from VFM directly. Wu *et al.* [58], on the other hand, leverage the pre-aligned textual embedding from CLIP as the middle ground for multi-modal feature alignment.

Despite the effectiveness of MM-UDA methods, they inevitably require full access to the source domain, which could be infeasible due to different factors, such as privacy or license concerns. To overcome this limitation, some primary works propose MM-TTA and MM-SFDA, which perform adaptation using backbones pre-trained on the source domain only. Specifically, SUMMIT [45] proposes the first MM-SFDA method by estimating cross-modal prediction agreement, yet it requires multiple offline training epochs. MM-TTA [44] is a more flexible and efficient pipeline, which conducts online adaptation as the existing online TTA methods. Shin *et al.* [44] propose the first MM-TTA method, which adaptively attends to the modality with less prediction entropy in a point-wise manner. However, all existing MM-UDA, MM-SFDA, and MM-TTA methods focus on the refinement of single-scan prediction while neglecting the correlations between geometric nearest neighbors. In this work, we propose Latte/Latte++ to leverage these informative correspondences that naturally exist for better modal-wise reliability estimation and more effective cross-modal attending.

**Temporal processing of point clouds.** Since point clouds are naturally in the form of temporally consecutive frames, previous methods have widely explored how to leverage such temporal information for different tasks. Specifically, scene flow [24], [50], [52], [53] contains the movement of every point in the 3D world. Considering such point-wise computation expensive, previous works on different tasks (*e.g.*, segmentation [9], [11], [43] and object detection [40]) usually interpret the temporal information from a simpler perspective. In terms of fully supervised learning, Choy *et al.* [11] propose the first 4D segmentation method by generalized sparse convolution kernels [21] and Fan *et al.* [15] turn to the fully connected learning scheme as in [41], while Xu *et al.* [62] extract long-term temporal information by an efficient memory bank. On the other hand, considering scenarios with insufficient or zero annotations, some works

<sup>1</sup>As our discussion mainly lies in online adaptation, “TTA” refers to online TTA methods in this work for simplicity

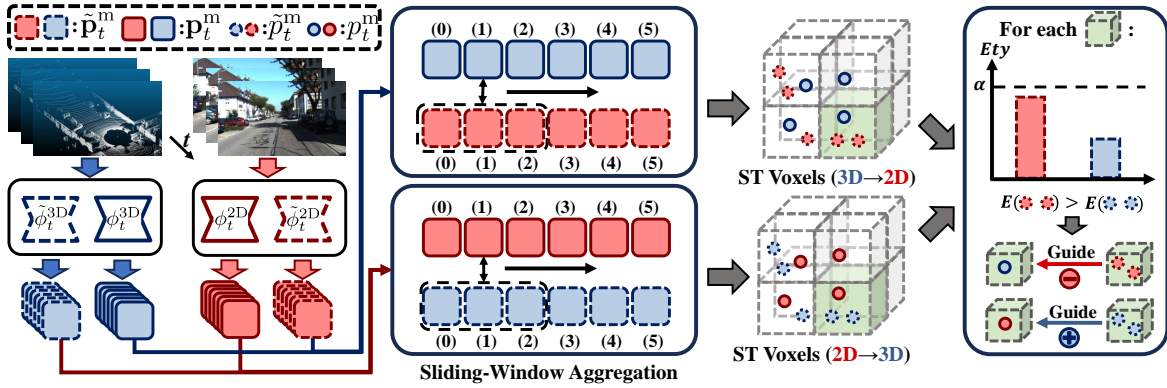


Fig. 2. Overall structure of Latte. Taking a student prediction frame of one modality as the query input, our sliding-window aggregation searches its spatial-temporal correspondences through voxelization within a time window to establish the temporally local prediction consistency. ST voxels are then generated, where those with high ST entropy (larger than  $\alpha$ -quantile) are discarded as unreliable correspondences, while the others are leveraged for adaptive cross-modal learning by attending to the modality with lower ST entropy in a voxel-wise manner.

propose different strategies to couple spatial-temporal information without ground-truth labels. For instance, Chen *et al.* [9] proposes to guide voxelized spatial-temporal representation with strong text embedding from CLIP [42] instead of labels in a multi-modal manner, while Saltor *et al.* [43] interpret such representation by nearest neighbor search in a frame-to-frame manner. In this work, we design sliding-window aggregation and voxelization rather than aggregating all frames as in [9], which better indicates the point-wise prediction reliability.

### III. METHODOLOGY

**Problem definition.** During MM-TTA for 3D segmentation, both 2D RGB images and 3D point clouds are captured consecutively in the target domain  $\mathcal{T}$ , denoted as  $\mathbf{x}_{\mathcal{T},t}^{2D} \in \mathbb{R}^{3 \times H \times W}$  and  $\mathbf{x}_{\mathcal{T},t}^{3D} \in \mathbb{R}^{N \times 4}$ , respectively, where  $t$  represents the frame order and  $H, W$  are the height and width of input images. The point-wise input contains the 3D coordinate  $\{x, y, z\}$  and the point feature (*e.g.*, intensity, reflectivity, etc.). Modality-specific networks are pre-trained on the labeled source domain before adaptation, denoted as  $\phi_{\mathcal{T},t}^m(\cdot)$  with  $m \in \{2D, 3D\}$ . During MM-TTA, both networks are initialized from the parameters pre-trained on the source domain. Following previous works [25], [44], 3D points are projected to the 2D image based on the relative projection matrix to obtain cross-modal correspondences within each frame, resulting in the modality-specific predictions  $\mathbf{p}_{\mathcal{T},t}^m = \phi_{\mathcal{T},t}^m(\mathbf{x}_{\mathcal{T},t}^m)$ ,  $\mathbf{p}_{\mathcal{T},t}^m \in \mathbb{R}^{N \times K}$  where  $K$  denote the number of semantic classes. Raw data from the labeled source domain are strictly inaccessible and we omit the target domain subscript  $\mathcal{T}$  by default.

The multi-modal input of online 3D segmentation is temporally consecutive, which exhibits strong temporal relationships between frames. The geometric neighborhoods across frames can be viewed as the various observations on the same semantic object that can be leveraged to stabilize noisy single-frame predictions. Motivated by this observation, we develop **Latte** and **Latte++**, which discover reliable spatial-temporal (ST) correspondences to improve both optimization stability and prediction consistency during MM-TTA. As shown in Fig. 2, given consecutive frames of 2D images and 3D point clouds as

input, Latte and Latte++ firstly extract their frame-wise predictions from both student and teacher networks (Sec. III-A). The predictions are then passed to the sliding-window aggregation and voxelization (Sec. III-B). Latte subsequently computes ST voxels and ST entropy that indicate the prediction consistency and certainty (Sec. III-C), while Latte++ leverages different corresponding under various aggregated frames to generate more informative ST voxels and entropy for reliability estimation (Sec. III-D). The final ST entropy is leveraged for cross-modal attending to alleviate the noise from unreliable modality-specific predictions (Sec. III-E).

#### A. Frame-wise Predictions from Students and Teachers

Before exploiting spatial-temporal correspondence, we first generate the frame-wise predictions from each modality. Motivated by the fact that moving average models can provide more stable online predictions [7], [49], [56], both Latte and Latte++ utilize weight-averaged teacher models and fast student models for each modality, denoted as  $\tilde{\phi}_t^m(\cdot)$  and  $\phi_t^m(\cdot)$ , respectively. Given each input frame  $\mathbf{x}_t^m$ , the student predictions  $\mathbf{p}_t^m$  and teacher predictions  $\tilde{\mathbf{p}}_t^m$  are computed as:

$$\tilde{\mathbf{p}}_t^m = \tilde{\phi}_t^m(\mathbf{x}_t^m), \mathbf{p}_t^m = \phi_t^m(\mathbf{x}_t^m), \quad (1)$$

where the teacher model  $\tilde{\phi}_t^m$  is initialized from the source domain pre-trained models. In the following process, the teacher's predictions of one modality are regarded as the cross-modal guidance of student predictions from the other modality. In practice, the gradient propagation of teacher model predictions is discarded to prevent directly updating teacher models.

#### B. Sliding-Window Aggregation and Voxelization

Our goal is to efficiently leverage spatial-temporal correspondences between predictions and seek reliability estimation through prediction consistency within correspondences. Establishing spatial-temporal correspondences in 3D space has been explored in other deep learning tasks, where they mainly consider temporally global relationships of all input frames [9], [43] or frame-to-frame correspondences [43]. However, they



both have some limitations in terms of consistency and certainty evaluation: the former can not highlight the risk of some inconsistent predictions within a short time window (*i.e.*, temporally local inconsistency), while the latter suffers from an insufficient number of correspondences.

To effectively empower spatial-temporal information with Latte and Latte++, we propose a sliding-window aggregation that focuses on temporally local correspondences that lie within a time window to evaluate local consistency temporally. Specifically, given a student prediction frame  $\mathbf{p}_i^m$  with the temporal index  $i$  as the query, the correspondence search is conducted within a time window of consecutive frames denoted as  $\{j | |j - i| \leq w_t\}$ , where  $w_t$  is the pre-defined time window size. The merged point cloud  $\hat{\mathbf{x}}_i^{3D} \in \mathbb{R}^{\hat{N} \times 3}$  (point features are omitted for simplicity) for correspondence search is then formulated as:

$$\hat{\mathbf{x}}_i^{3D} = \text{cat}(\{\mathbf{T}_{j \rightarrow i} * \mathbf{x}_j^{3D} | |j - i| \leq w_t\}), \quad \mathbf{T}_{j \rightarrow i} = \mathbf{T}_i^{-1} \mathbf{T}_j, \quad (2)$$

where  $\mathbf{T}_i$  is the estimated pose at frame  $i$  and so as  $\mathbf{T}_j$ , which can be easily obtained online through off-the-shelf SLAM algorithms [26], [51].  $\text{cat}(\cdot)$  is the concatenation operation along the point number dimension while  $*$  denotes the pose transformation. The voxelization is then performed on  $\hat{\mathbf{x}}_i^{3D}$ , formulated as:

$$\mathbf{v}_i^{3D} = \mathcal{V}_s(\hat{\mathbf{x}}_i^{3D}), \quad \mathbf{v}_i^{3D} \in \mathbb{R}^{\hat{N}_v \times 3}, \quad (3)$$

$$\mathbf{M}_i^{3D} = \{k | \forall g \in [1, \hat{N}], [\hat{\mathbf{x}}_{i,g}^{3D} / \mathbf{s}] = \mathbf{v}_{i,k}^{3D}\}, \quad \mathbf{M}_i^{3D} \in \mathbb{R}^{\hat{N}}, \quad (4)$$

where  $\mathbf{v}_i^{3D}$  is the extracted voxels and  $\mathcal{V}_s$  is the voxelization operation with a voxel size  $\mathbf{s}$ . After voxelization, points located in the same voxel can be regarded as correspondences since they are geometric neighborhoods, where the hash table  $\mathbf{M}_i^{3D}$  that maps each voxel back to its containing points (*e.g.*,  $\mathbf{v}_{i,k}^{3D}$  to  $\hat{\mathbf{x}}_{i,g}^{3D}$  as in Eq. (4)) is preserved for the subsequent correspondence mapping. In this way, it provides more diverse neighborhood selection strategies with temporally local correspondences for consistency and certainty evaluation compared to globally merging all frames in one single step. In practice, the sliding-window aggregation and voxelization are conducted iteratively for each frame in the input batch.

### C. Spatial-Temporal Voxels and Entropy

Given the geometric correspondences captured by voxelization, our goal is to emphasize the predictions with correspondence consistency within each voxel. After sliding-window aggregation and voxelization, there inevitably exist some unreliable correspondences of two different types: (i) voxels that contain different types of semantic objects (*e.g.*, those located on the contact surface between cars and roads) and (ii) voxels with highly inconsistent predictions due to uncertain predictions across time. These unreliable correspondences contain high uncertainty and inconsistency, which could harm the on-line optimization of models if they as references. To alleviate the side-effect introduced by such unreliable correspondences, we propose ST voxels that leverage ST entropy for voxel-wise reliability evaluation and cross-modal attending.

Specifically, an ST voxel contains two components, including the query and the reference, where the query is

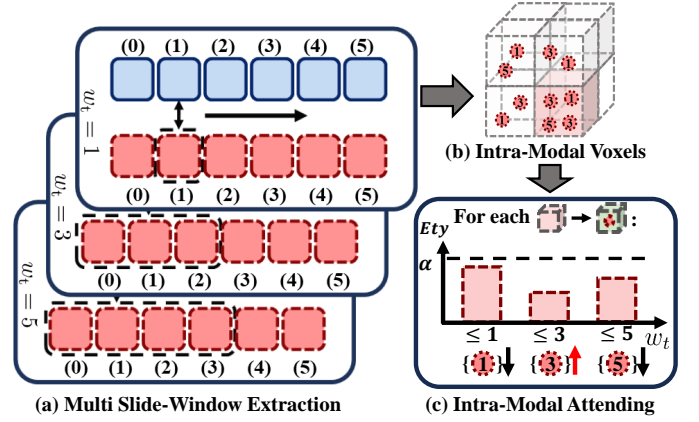


Fig. 3. Illustration of multi-window aggregation and intra-modal attending. Here we take 2D as reference predictions for exemplary presentation, where the digit of each circle indicates the smallest time window introducing this point/pixel in this voxel. For each modality, multi-window extraction leads to different point/pixel combinations within each voxel, providing a more informative reliability estimation of each modality.

encouraged to be consistent with the reference. Considering that the moving average teacher can usually generate more stable predictions [7], [56], we regard the single-frame student predictions as the query while multi-frame teacher predictions as our reference, forming ST voxels denoted as  $\mathbf{v}_i^{ST}$ . Without losing generality, here we take a single ST voxel indexed by  $k$  in frame  $i$  as an example, denoted as  $\mathbf{v}_{i,k}^{ST} = \{\mathbf{p}_q^m, \mathbf{p}_r^m\}$ , where  $\mathbf{p}_q^m \in \mathbb{R}^{\hat{N}_q \times K}$  and  $\mathbf{p}_r^m \in \mathbb{R}^{\hat{N}_r \times K}$  are the point-wise student predictions at the query frame  $i$  and teacher predictions in the frame searching range  $j$ , respectively, formulated as:

$$\mathbf{p}_q^m = \{\mathbf{p}_{i,g}^m | [\hat{\mathbf{x}}_{i,g}^{3D} / \mathbf{s}] = \mathbf{v}_{i,k}^{3D}\}, \quad (5)$$

$$\mathbf{p}_r^m = \{\tilde{\mathbf{p}}_{j,g}^m | [\hat{\mathbf{x}}_{j,g}^{3D} / \mathbf{s}] = \mathbf{v}_{i,k}^{3D}, |j - i| \leq w_t\}, \quad (6)$$

The reliability of each voxel is then evaluated as the Shannon's entropy [59] of the average teacher predictions, where the unreliable ST voxels are then filtered out given a pre-defined quantile  $\alpha$  as in Fig. 2, denoted as:

$$E_{i,k}^m = - \sum_c^K \bar{\mathbf{p}}_{r,c}^m \log \bar{\mathbf{p}}_{r,c}^m, \quad \bar{\mathbf{p}}_r^m = \sum_{n=1}^{N_r} \psi(\mathbf{p}_{r,n}^m) / N_r, \quad (7)$$

$$h_{i,k} = \begin{cases} 0, & \text{if } E_{i,k}^m > Q^m(\alpha) \\ 1, & \text{if } E_{i,k}^m \leq Q^m(\alpha) \end{cases}, \quad (8)$$

where  $E_{i,k}^m$  is regarded as the ST entropy of voxel  $k$  for modality  $m$ , indicating the modal-specific prediction reliability within this voxel.  $Q^m(\alpha)$  is the  $\alpha$ -quantile of all ST entropy in modality  $m$  in the same batch and  $\psi(\cdot)$  denotes the Softmax function along the class dimension.

### D. Multi-Window Aggregation and Intra-Modal Attending

The vanilla Latte evaluates the modal reliability through the local prediction consistency within a pre-defined universal window size  $w_t$ , while the optimal  $w_t$  for consistency evaluation might vary among different semantic objects. For instance, highly dynamic objects are better evaluated with a short window to avoid incorrect correspondences due to the

shadow-like effect, while the local prediction inconsistency of static backgrounds can be effectively suppressed by enlarging the time window and introducing more correspondences. To overcome this limitation, we propose Latte++ to generate the reference predictions and ST entropy by considering frame aggregations with different sliding window sizes.

Specifically, instead of using a single sliding window size  $w_t$ , we define a set of  $N_t$  available window sizes denoted as  $\mathbf{w}_t = \{w_d\}_{d=1}^{N_t}$ . Aggregation and voxelization (Eq. (2-4)) are conducted with each  $w_d \in \mathbf{w}_t$  in the same voxelization grid. As a result, each voxel corresponds to a set of reference predictions  $\{\mathbf{p}_{r,d}^m\}_{d=1}^{N_t}$  (Eq. (6)) and their corresponding ST entropy  $\{E_{i,k,d}^m\}_{d=1}^{N_t}$  (Eq. (7)), where  $d$  corresponds to the time window index. The resulting set of reference predictions contains various spatial-temporal correspondences lying within different time windows. Thus its corresponding ST entropy provides a more informative reliability estimation compared to using a single sliding window as in Latte. To gather the estimation from different time windows, we designed an intra-modal weighting mechanism before cross-modal interaction to attend the reference predictions with less ST entropy, formulated as:

$$E_{i,k}^m = \sum_t h_{i,k,d} \tau_d^m E_{i,k,d}^m, \quad \bar{\mathbf{p}}_r^m = \sum_d h_{i,k,d} \tau_d^m \bar{\mathbf{p}}_{r,d}^m, \quad (9)$$

$$\tau_d^m = \frac{h_{i,k,d} \tau_d^b \exp(E_{i,k,d}^m)}{\sum_d h_{i,k,d} \tau_d^b \exp(E_{i,k,d}^m)}, \quad (10)$$

$$h_{i,k,d} = \begin{cases} 0, & \text{if } E_{i,k,d}^m > Q^m(\alpha) \\ 1, & \text{if } E_{i,k,d}^m \leq Q^m(\alpha) \end{cases}, \quad (11)$$

where  $\tau_d^m$  is the window weight computed based on the predefined initial weight  $\tau_d^b$  and its corresponding ST entropy  $E_{i,k,d}^m$ . Since the long-term prediction consistency exhibits more confidence in prediction consistency than the short-term ones, we introduce an initial weight  $\tau_d^b$  (here we empirically set  $\tau_d^b = \log_2(2 + w_d)$ ) which is positively related to the window size. The  $\alpha$ -quantile filtering is also introduced in Eq. (11) to filter out the extremely noisy candidates before our intra-modal attending. Note that  $Q^m(\alpha)$  here is computed based on all ST entropy from different window sizes. The valid index in Eq. (8) is subsequently re-formulated as:

$$h_{i,k} = \begin{cases} 0, & \text{if } \forall d, h_{i,k,d} = 0 \\ 1, & \text{if } \exists d, h_{i,k,d} = 1 \end{cases}. \quad (12)$$

### E. ST Voxel Aided Cross-Modal Learning

Each modality has its pros and cons under different conditions and cross-modal learning for online scenarios should therefore possess an adaptive mechanism that attends to the ‘‘pros’’ while suppressing the ‘‘cons’’. To achieve that, Latte and Latte++ perform cross-modal learning by attending to the modality with more consistent and certain predictions from a spatial-temporal perspective. Specifically, taking ST voxel  $\mathbf{v}_{i,k}^{\text{ST}}$  and its corresponding ST entropy  $E_{i,k}^m$  as an example, the

---

### Algorithm 1: Adaptation and Online Prediction Process of Latte ((a-c), (f-h)) and Latte++ ((a), (d-h))

---

**Target Domain:** Multi-modal input  $\mathcal{X}_T = \{(\mathbf{x}_t^{2D}, \mathbf{x}_t^{3D})\}$ .  
**Init Model:**  $\hat{\phi}_t^m, \phi_t^m, m \in \{2D, 3D\}$ , window sizes  $\mathbf{w}_t$ .  
**for**  $\mathbf{x} = \{(\mathbf{x}_t^{2D}, \mathbf{x}_t^{3D})\}_{t=t_0+1}^B \in \mathcal{X}_T$  **do**  
  (a) Compute  $\hat{\mathbf{p}}_t^m, \mathbf{p}_t^m$  by Eq. (1).  
  **for**  $i \in [t_0 + 1, t_0 + B]$  **do**  
    **if**  $|\mathbf{w}_t| == 1$  **then**  
      (b) Compute  $\hat{\mathbf{x}}_i^{3D}, \mathbf{v}_i^{3D}, \mathbf{M}_i^{3D}$  within  $w_t$  by Eq. (2)-(4).  
      (c) Compute  $\mathbf{v}_i^{\text{ST}}$  and  $E_i^m$  by Eq. (5)-(8).  
    **else**  
      **for**  $w_d \in \mathbf{w}_t$  **do**  
        (d) Compute  $E_{i,k,d}^m, \mathbf{p}_{r,d}^m$  in  $w_d$  by Eq. (2)-(6).  
      **end**  
      (e) Compute  $E_i^m, \bar{\mathbf{p}}_r^m, h_{i,k}$  by Eq. (9)-(12).  
    **end**  
  **end**  
  (f) Compute  $\mathcal{L}_i^{\text{XM}}$  by Eq. (13)-(14).  
  (g) Compute  $\hat{E}_r^m$  and  $\mathbf{y}_r^{\text{XM}}$  by Eq. (15)-(17)  
  (h) Compute  $\mathcal{L}$  by Eq. (18) and update with Eq. (19)  
**end**

---

voxel-wise cross-modal attending weights and the weighted cross-modal consistency loss  $\mathcal{L}_{i,k}^{\text{XM}}$  are computed as:

$$w_v^{2D} = \frac{\exp(E_{i,k}^{2D})}{\exp(E_{i,k}^{2D}) + \exp(E_{i,k}^{3D})}, \quad w_v^{3D} = 1 - w_v^{2D}, \quad (13)$$

$$\mathcal{L}_{i,k}^{\text{XM}} = w_v^{2D} D_{\text{KL}}(\bar{\mathbf{p}}_q^{3D} \parallel \bar{\mathbf{p}}_r^{2D}) + w_v^{3D} D_{\text{KL}}(\bar{\mathbf{p}}_q^{2D} \parallel \bar{\mathbf{p}}_r^{3D}), \quad (14)$$

where  $D_{\text{KL}}(\cdot)$  represents the KL-divergence between two probability.  $\bar{\mathbf{p}}_q^{3D}$  is the average query predictions in the ST voxel, similarly computed as in Eq. (7).

The voxel-wise cross-modal attending is further extended to the point level for better online predictions and cross-modal pseudo-label generation. Specifically, the ST entropy is propagated from the ST voxel to its reference point-wise prediction, indicating its confidence and consistency within its spatial-temporal neighborhoods. If one’s ST entropy has been filtered out as in Eq. (8), its ST entropy would fall back to the point-level entropy. For an arbitrary point predictions  $\mathbf{p}^m \in \mathbf{p}_r^m$ , the cross-modal predictions  $\mathbf{y}^{\text{XM}}$  are formulated as:

$$\hat{E}_r^m = h_{i,k} E_{i,k}^m - (1 - h_{i,k}) \sum_c^K \mathbf{p}_c^m \log \mathbf{p}_c^m, \quad (15)$$

$$w_p^{2D} = \frac{\exp(\hat{E}^{2D})}{\exp(\hat{E}^{2D}) + \exp(\hat{E}^{3D})}, \quad w_p^{3D} = 1 - w_p^{2D}, \quad (16)$$

$$\mathbf{p}^{\text{XM}} = w_p^{2D} \mathbf{p}^{2D} + w_p^{3D} \mathbf{p}^{3D}, \quad \mathbf{y}^{\text{XM}} = \arg \max_c \mathbf{p}_c^{\text{XM}}. \quad (17)$$

### F. Online Predictions and Optimization

As shown in Fig. 2, given a batch of  $B$  consecutive frames  $\{\mathbf{x}_t^m\}_{t=t_0+1}^{t_0+B}$  as input, we first extract the student and teacher predictions through Eq. (1). Subsequently, frames are aggregated and voxelized as in Eq. (2), resulting in a batch of merged point cloud  $\{\hat{\mathbf{x}}_t^{3D}\}_{t=t_0+1}^{t_0+B}$  and voxels  $\{\mathbf{v}_t^{3D}\}_{t=t_0+1}^{t_0+B}$ . The ST voxels and ST entropy computation process is then applied to each frame of the merged point cloud and voxels. Due to the overlap of the sliding window, multiple ST entropy values could be propagated to the same point prediction, where we

empirically take the average value of all ST entropy received to proceed Eq. (15). The overall loss function and the updating scheme can be formulated as:

$$\mathcal{L} = \sum_t \mathcal{F}(\mathbf{p}_t^m, \mathbf{y}_t^{\text{xM}}) + \frac{\lambda_{\text{xM}}}{B} \sum_t \sum_k \mathcal{L}_{t,k}^{\text{xM}}, \quad (18)$$

$$\tilde{\theta}_t^m = \lambda_s \tilde{\theta}_{t-1}^m + (1 - \lambda_s) \theta_t^m, \quad (19)$$

where  $\mathcal{F}(\cdot)$  is the cross-entropy function and  $\mathbf{y}_t^{\text{xM}}$  is the point-wise cross-modal pseudo-label frame from Eq. (17), which is also regarded as our cross-modal prediction for evaluation.  $\theta_t^m$  and  $\tilde{\theta}_t^m$  are the model parameters of teacher and student models, respectively, where  $\lambda_s$  is the momentum update coefficient.  $\lambda_{\text{xM}}$  is pre-defined coefficient for the cross-modal consistency loss. Our adaptation and inference process is summarized in Algo. 1

#### IV. EXPERIMENTAL RESULTS

In this section, we present our thorough experimental results on three different benchmarks. Details of benchmarks, backbones, and settings are first present in Sec. IV-A. The main results are then illustrated in Sec. IV-B, followed by detailed ablation studies and qualitative results in Sec. IV-C.

##### A. Benchmarks and settings

**Benchmark Details.** To thoroughly investigate the effectiveness of Latte, we conduct our experiments on 3 different MM-TTA benchmarks, including (i) **USA-to-Singapore (U-to-S)**, (ii) **A2D2-to-SemanticKITTI (A-to-K)**, and (iii) **SynthIA-to-SemanticKITTI (S-to-K)**. Specifically, U-to-S is developed from NuScenes-LiDARSeg [4] dataset, where the domain gap is mainly credited to the infrastructure difference between countries. Same as [25], the source domain and the target domain data are selected by filtering country keywords based on the data recording description in NuScenes. Different from previous UDA methods [25], [38] utilizing self-defined class mappings, we follow the official mapping in NuScenes-LiDARSeg, forming a 16-class segmentation benchmark. The remaining two benchmarks follow a similar setting as in [44], where the domain gap of A-to-K [2], [17] lies in different LiDAR mounting positions and image resolutions while the one of S-to-K [2] lies in different patterns between synthetic and real data for both modalities. For A-to-K, we adopt the same class-mapping as in [25], [44] which leads to a 10-class benchmark, while we design our class-mapping for S-to-K since its original class map has not been revealed previously [44], forming a 9-class benchmark. *More details are presented in our appendix.*

In addition to the standard MM-TTA benchmarks with stationary target domains, we further extend our comparison to its more challenging variant, named Multi-Modal Continuous Test-Time Adaptation (MM-CTTA), where the target domain is continuously changing with different weathers or illumination conditions [7], [56]. Specifically, we leverage the two MM-CTTA benchmarks for 3D segmentation proposed in [7], including **SemanticKITTI-to-Synthia (K-to-S)** and **SemanticKITTI-to-Waymo (K-to-W)**, where the former one is a challenging synthetic-to-real benchmark with large domain

discrepancy while the latter is less challenging but closer to real-life deployment. Both benchmarks are preprocessed and organized following the identical protocol as in [7].

**Baseline methods.** Previous TTA and MM-TTA methods are included in comparison with Latte/Latte++. For TTA methods, we compare Latte and Latte++ with point-wise pseudo-labels with filtering (PsLabel), TENT [54], ETA [36], SAR [37] with and without restoring (denoted as SAR-rs and SAR, respectively). MMTA [44] as well as its online version of xMUDA [25] (including pure xMUDA and pseudo-label version xMUDA<sub>PL</sub>) are additionally included as the previous SOTA methods for comparison. Considering that EATA [36] with Fisher regularizer requires pre-access to the target domain samples, we compare Latte with ETA, an official variant of EATA without this regularizer for a fair comparison. Since our extended evaluation involves a new challenging scenario MM-CTTA, two SOTA CTTA methods (CoTTA [56] and CoMAC [7]) based on multiple augmented predictions are additionally introduced to justify our effectiveness and efficiency under different MM-TTA settings. We further present a performance lower bound by directly testing with source pre-trained models (*i.e.*, Source only) and an upper bound by online adapting networks with ground-truth labels from the target domain for one epoch (*i.e.*, Oracle TTA).

**Implementation details.** With the rapid progress in 2D and 3D segmentation, we employ all baseline methods and Latte/Latte++ with more recent SegFormer [60] (SegFormer-B1) and SPVCNN [48] (SPVCNN-cr1) as their 2D and 3D backbones, respectively, to investigate the improvement of existing TTA methods when combined with advanced networks. The pre-training procedures on the source domain follow a similar setting as in [25], except for 2D SegFormer which is trained with a base learning rate of 6E-5 with an AdamW optimizer and Poly scheduler as in [60]. For Latte, we maintain the same learning rate and optimizer as in the pre-training stage, while the scheduler is disabled. For our voxelization, we leverage the off-the-shelf SLAM algorithm KISS-ICP [51] to generate poses and utilize a window size  $w_t$  of 3 with a voxel size of 0.2m, while the quantile  $\alpha$  and coefficient  $\lambda_{\text{xM}}$  are set to 0.9 and 0.3, respectively.  $\lambda_s$  is empirically set to 0.99 as in [7], [46]. The window sizes of Latte++  $\mathbf{w}_m$  are set to [3, 5]. For all methods, we strictly follow the *one-pass* protocol to first evaluate the predictions of the input batch and then update the networks. For most baseline and Latte/Latte++, we follow previous works [36], [54] to update only the trainable parameters in normalization layers, while CoTTA and CoMAC are used to update all trainable parameters as stated in their original protocols [7], [56]. For all baselines, we conduct a parameter search and report their best results. We utilize the mean intersection over union (mIoU) as our evaluation metric. All experiments are conducted with PyTorch on a single RTX 3090. *More details are included in appendices.*

##### B. Overall Results

1) *Results on MM-TTA benchmarks:* Tab. I presents the overall results of our Latte on three benchmarks compared with previous SOTA methods. In terms of average cross-modal

TABLE I

PERFORMANCE (mIOU) COMPARISON OF LATTE ON MM-TTA BENCHMARKS. LATTE/LATTE++ OUTPERFORMS ALL PREVIOUS SOTA METHODS ON THE CROSS-MODAL METRIC (xM) ACROSS THREE BENCHMARKS. HERE “MM” DENOTES WHETHER THE MULTI-MODAL INTERACTION IS USED OR NOT. “AVG” PRESENTS THE AVERAGE xM PERFORMANCE ACROSS THREE BENCHMARKS. “INF. TIME” IS COMPUTED AS THE AVERAGE INFERENCE TIME OF THREE BENCHMARKS.

Method	Publication	MM	Inf. Time (ms)	U-to-S			A-to-K			S-to-K			Avg
				2D	3D	xM	2D	3D	xM	2D	3D	xM	
Source only	-	✗	52.7	31.4	41.1	43.9	47.4	17.9	44.3	23.4	36.4	38.2	42.1
Oracle TTA	-	✗	184.7	38.7	45.5	50.3	49.1	61.3	62.5	36.0	54.5	54.6	55.8
TENT [54]	ICML-21	✗	154.6	36.8	36.1	41.1	43.3	44.4	49.1	22.4	35.5	37.5	42.6
ETA [36]	ICML-22	✗	65.5	36.7	34.7	43.7	43.2	42.5	49.7	22.4	30.6	32.9	42.1
SAR [37]	ICLR-23	✗	270.0	36.6	37.2	43.9	43.0	42.7	50.3	20.7	31.3	32.9	42.4
SAR-rs [37]	ICLR-23	✗	271.2	36.6	35.5	43.9	43.1	43.8	50.1	24.2	25.1	28.8	40.9
xMUDA [25]	PAMI-22	✓	168.0	19.4	22.9	24.2	13.1	33.0	32.2	12.2	14.8	14.1	23.5
xMUDA <sub>PL</sub> [25]	PAMI-22	✓	168.7	36.2	38.2	43.0	42.8	48.3	50.9	30.9	34.1	36.3	43.4
MMTTA [44]	CVPR-22	✓	184.3	37.2	<b>41.5</b>	45.4	44.5	51.7	53.7	27.5	35.1	35.5	44.9
CoTTA [56]	CVPR-22	✓	989.6	37.0	34.5	43.7	46.0	42.2	50.5	30.7	35.1	35.6	43.3
CoMAC [7]	ICCV-23	✓	995.7	37.3	35.6	42.7	43.5	42.8	51.5	25.3	30.2	32.4	42.2
PsLabel	-	✓	183.3	<b>37.7</b>	35.8	41.8	<b>46.7</b>	44.3	50.0	29.2	33.3	35.3	42.4
TENT+xM [54]	ICML-21	✓	155.3	37.1	39.7	45.2	43.3	47.1	50.3	23.9	36.5	37.7	44.4
ETA+xM [36]	ICML-22	✓	67.0	36.9	35.2	44.8	43.1	44.2	50.1	23.7	30.8	33.1	42.7
SAR+xM [37]	ICLR-23	✓	270.1	36.9	39.4	45.5	43.1	46.3	50.5	22.8	32.8	34.5	43.5
SAR-rs+xM [37]	ICLR-23	✓	272.1	36.9	36.8	45.0	43.1	45.6	50.5	23.8	30.7	33.1	42.9
<b>Latte (Ours)</b>	-	✓	221.1	37.5	<u>41.0</u>	<u>46.2</u>	46.0	<u>52.5</u>	<u>54.2</u>	<u>33.3</u>	<u>39.3</u>	<u>41.7</u>	<u>47.3</u>
<b>Latte++ (Ours)</b>	-	✓	242.2	<u>37.6</u>	<u>41.0</u>	<b>46.3</b>	<u>46.4</u>	<b>53.0</b>	<b>55.1</b>	<b>33.5</b>	<b>39.9</b>	<b>42.5</b>	<b>48.0</b>

predictions (Avg), Latte surpasses all previous TTA or MM-TTA methods, with a significant relative improvement of more than 5.3%. For the less challenging U-to-S and A-to-K (*i.e.*, gap between Oracle TTA and best TTA less than 10%), Latte achieves consistent relative improvements of 1.3% on U-to-S and 1.1% on A-to-K compared to MMTTA, respectively. By leveraging the consistency checks from various time windows, Latte++ further expands the relative performance gaps to about 2% on U-to-S and 2.6% on A-to-K in comparison with MMTTA. On the contrary, most existing methods except for xMUDA [25] can achieve superior performance compared to source-only results when one modality is reliable as in U-to-S (3D prevails) and A-to-K (2D prevails).

In terms of the most challenging S-to-K, Latte exhibits significant performance improvement compared to previous SOTA MM-TTA methods such as MMTTA [44] and xMUDA<sub>PL</sub> [25], with a relative gap of 14.6%. In fact, all previous methods except for our Latte and Latte++ perform inferiorly compared to source pre-trained models (Source only), due to the significant domain gaps caused by the non-trivial pattern difference in both modalities between synthetic and real data. In this case, the instability of single-frame predictions becomes exacerbated, leading to performance degeneration in MMTTA which mainly relies on single-frame refinement. This justifies the effectiveness of Latte under either challenging or less challenging TTA scenarios. Additionally, the consistent gap across all evaluation metrics (*i.e.*, “2D”, “3D”, or “xM”) between Latte++ and Latte justifies the benefit of using various time windows. Another interesting observation is that almost all cross-modal methods outperform other single-modal TTA methods, *e.g.*, even the simplest PsLabel can outperform recent TTA methods like SAR [37]. This reveals the non-trivial benefits of cross-modal learning for TTA with segmentation. To provide a fair comparison, we thus supplement the results with existing TTA methods combined with a widely used cross-modal learning scheme xMUDA [25]

as in Tab. I. Specifically, the cross-modal prediction consistency loss from [16] is included for each TTA method as their additional optimization objective with a coefficient of 0.1. Although the cross-modal learning scheme brings an average relative improvement of 1.0-4.0%, the performance gap between existing TTA methods and Latte/Latte++ is still non-trivial, which justifies the superiority of our cross-modal learning scheme in Latte/Latte++.

2) *Results on MM-CTTA benchmarks:* We further evaluate the performance of Latte and Latte++ on MM-CTTA benchmarks with continuously changing target domains. As shown Tab. II, when testing on K-to-S which initially possesses more challenging synthetic-to-real domain discrepancy, both Latte and Latte++ yield noticeable relative improvements of 3.6% and 4.9% on the average cross-modal segmentation performance compared to existing SOTA method xMUDA<sub>PL</sub>, respectively. For sequence-wise performance, they outperform the single-scan refinement method MMTTA by at least 5.0% on 8/12 sequences. When evaluated on the less challenging K-to-W, Latte performs competitively with a trivial relative gap of less than 0.2% compared to xMUDA<sub>PL</sub>, while Latte++ achieves SOTA performance of 50.7% by leveraging the more informative multi-window aggregation. Similar to K-to-S, both Latte and Latte++ surpass the sequence-wise performance of MMTTA on all sequences in K-to-W, leading to a significant overall improvement of 5.5%. Following the experimental settings in CoMAC [7], we conduct additional runs with Latte/Latte++ and existing SOTA methods (xMUDA<sub>PL</sub>, MMTTA, PsLabel) by reversing the sequence playback order of these two benchmarks for a more thorough comparison. Despite the non-trivial universal performance degeneration caused by the more challenging setting (*i.e.*, TTA begins with the sequences with large initial domain gaps, such as 05-Rain and N-2), the gap between Latte/Latte+ and the existing SOTA TTA/MMTTA methods remain consistent on both benchmarks, which further justify the effectiveness of our

TABLE II  
CROSS-MODAL PERFORMANCE (mIOU) COMPARISON OF LATTE ON MM-CTTA BENCHMARKS. HERE WE REPORT THE SOFTMAX-AVERAGE mIOU OF 2D AND 3D PREDICTION.

Time	t →												t ←											
	SemanticKITTI-to-Synthia (K-to-S)												SemanticKITTI-to-Waymo (K-to-W)											
Methods	01-Spring	02-Summer	04-Fall	05-Winter	01-Dawn	02-Night	04-Sunset	05-W-night	01-Fog	02-S-Rain	04-R-Night	05-Rain	xM Avg	D-O-1	D-P-1	D-S-1	DD-1	N-1	D-O-2	D-P-2	D-S-2	DD-2	N-2	xM Avg
	Source	48.0	35.1	43.0	36.8	46.3	29.9	41.4	33.4	49.3	26.4	36.8	29.4	38.0	43.5	45.9	46.1	42.8	38.3	43.6	48.1	44.9	45.1	37.1
Oracle	50.0	47.0	56.0	51.6	54.9	55.1	58.3	53.8	56.0	53.0	57.7	48.1	53.5	46.0	49.7	49.0	47.8	46.3	51.4	53.3	49.9	51.1	47.2	49.2
TENT	45.6	33.8	42.4	38.2	44.7	32.1	41.3	35.2	45.8	27.5	32.7	32.3	37.6	43.9	35.7	42.4	41.2	39.0	42.1	48.0	38.9	41.7	38.7	42.2
ETA	45.1	32.7	42.5	36.8	43.9	30.0	41.6	32.4	39.9	26.3	31.3	27.4	35.8	43.9	46.6	43.3	42.1	38.5	44.7	50.2	42.0	44.5	39.0	43.5
SAR	45.1	32.9	42.3	37.6	44.6	31.9	42.1	34.9	46.0	27.8	33.1	31.4	37.5	44.0	46.5	43.5	42.0	39.3	44.4	50.0	41.6	44.2	39.8	43.5
SAR-rs	45.0	32.9	42.4	37.2	44.1	30.7	41.9	33.6	44.6	27.1	32.7	29.5	28.8	44.0	46.6	43.5	41.9	38.5	44.6	50.3	41.8	44.1	38.4	43.4
xMUDA	45.6	24.0	31.2	19.5	25.9	16.6	23.6	18.6	25.3	14.4	19.7	16.0	23.4	43.5	38.9	30.9	26.4	26.2	29.8	31.6	26.8	28.7	27.1	31.0
xMUDA <sub>PL</sub>	45.5	35.1	46.8	43.5	47.4	43.9	51.2	45.8	47.9	40.6	44.5	43.7	44.7	44.6	48.4	47.5	48.1	51.3	51.3	53.0	50.3	53.4	53.8	50.2
MMTTA	46.2	36.4	48.4	45.7	47.3	42.5	52.0	46.6	49.5	37.7	41.4	41.4	44.2	44.1	45.2	44.6	43.8	43.1	43.8	48.0	45.4	47.4	47.0	45.2
PsLabel	45.4	34.8	46.1	42.4	46.3	42.4	49.7	43.9	46.3	40.0	43.6	42.5	43.6	44.7	48.8	47.4	48.2	50.9	51.0	53.0	49.8	53.0	53.2	50.0
CoTTA	47.3	36.4	46.6	40.7	41.7	40.5	49.4	41.4	45.0	40.8	44.2	40.2	42.8	47.3	36.4	46.6	40.7	41.7	40.5	49.4	41.4	45.0	40.8	44.2
CoMAC	47.4	37.2	47.0	44.3	46.5	37.2	48.5	42.2	49.1	24.2	28.3	18.5	39.2	44.2	45.7	44.0	41.9	35.2	41.5	42.8	40.5	40.4	28.2	40.4
<b>Latte</b>	46.6	41.3	51.5	46.6	47.3	48.5	53.8	48.3	47.7	42.2	44.3	37.2	46.3	44.5	48.3	47.5	47.9	50.5	51.2	53.8	50.3	53.8	53.7	50.1
<b>Latte++</b>	47.0	41.5	51.9	46.9	47.5	49.0	54.2	48.6	48.0	43.2	45.7	38.8	46.9	45.7	49.0	48.3	48.1	50.4	51.8	54.1	50.9	54.1	54.3	50.7
Time	t ←												t →											
xMUDA <sub>PL</sub>	46.3	43.4	50.7	44.0	46.2	39.7	45.9	36.7	44.7	28.6	32.6	27.2	40.5	48.2	49.7	49.9	48.6	50.9	48.9	51.1	43.6	44.8	38.8	47.4
MMTTA	48.9	46.9	51.5	46.7	46.9	40.2	44.8	34.0	42.4	24.0	30.6	26.0	40.2	45.8	46.5	49.9	47.7	50.8	50.3	50.7	46.0	45.7	39.6	47.3
PsLabel	45.4	41.0	49.6	42.4	45.2	38.2	45.0	36.2	44.5	28.9	32.8	27.4	39.7	47.3	50.1	49.5	48.2	50.6	48.4	51.4	43.6	45.1	39.7	47.4
<b>Latte</b>	47.9	46.1	51.6	45.1	46.5	42.7	47.1	38.4	46.1	28.3	32.8	27.2	41.6	48.7	49.9	50.2	48.4	50.6	49.2	51.7	44.0	45.0	39.6	47.7
<b>Latte++</b>	47.9	46.0	51.6	45.1	46.5	42.7	47.1	38.4	46.2	28.3	32.8	27.2	41.6	49.1	49.7	50.4	48.6	50.3	49.2	51.2	43.8	45.2	39.7	47.7

TABLE III  
CLASS-WISE PERFORMANCE (mIOU) COMPARISON ON A-TO-K.

Modality	Method	Car	Truck	Bike	Person	Road	Parking	Sidewalk	Building	Nature	O-Object	Avg
2D	xMUDA <sub>PL</sub>	69.2	23.4	29.6	23.2	85.1	9.5	56.7	48.8	58.3	24.2	42.8
	CoTTA	69.6	<b>30.9</b>	<b>35.2</b>	<b>29.9</b>	82.8	7.4	53.8	48.8	<b>75.8</b>	25.8	46.0
	Latte	70.6	30.1	31.4	25.5	85.5	8.0	56.7	50.3	72.3	29.3	46.0
	Latte++	<b>70.7</b>	30.5	31.9	<b>26.4</b>	<b>85.6</b>	8.1	<b>56.9</b>	<b>50.5</b>	73.8	<b>29.8</b>	<b>46.4</b> <sub>(+0.4)</sub>
3D	xMUDA <sub>PL</sub>	83.3	22.5	47.2	30.2	<b>89.5</b>	<b>12.1</b>	60.9	53.0	58.3	25.7	48.3
	CoTTA	67.9	13.4	43.9	26.8	83.4	8.1	51.0	39.3	64.0	24.4	42.2
	Latte	<b>83.4</b>	<b>36.8</b>	49.1	34.7	89.1	11.0	61.0	57.0	71.7	31.0	52.5
	Latte++	82.7	<b>36.8</b>	<b>49.5</b>	<b>36.0</b>	89.1	11.1	<b>61.2</b>	<b>57.5</b>	<b>73.8</b>	<b>32.3</b>	<b>53.0</b> <sub>(+0.5)</sub>
xM	xMUDA <sub>PL</sub>	<b>82.4</b>	30.5	<b>49.2</b>	36.2	<b>90.7</b>	<b>11.3</b>	<b>63.4</b>	56.5	62.0	27.2	50.9
	CoTTA	75.6	37.6	44.6	37.2	86.5	6.7	58.3	51.7	78.2	29.0	50.5
	Latte	80.1	43.7	48.1	36.7	90.0	9.1	63.0	59.2	77.4	34.3	54.2
	Latte++	80.4	<b>44.8</b>	48.9	<b>39.1</b>	90.1	9.3	<b>63.4</b>	<b>59.8</b>	<b>79.3</b>	<b>35.6</b>	<b>55.1</b> <sub>(+0.9)</sub>

method. It is worth noting that the performance gap between Latte and Latte++ becomes rather trivial when reversing the sequence order, mainly because there exists an increasing number of consistently incorrect predictions due to the large initial domain discrepancy. In this case, utilizing multiple time windows has limited contribution to stabilizing the intra-modal prediction noise, which leads to the similar performance of Latte and Latte++ when facing significant initial domain gaps in MM-CTTA.

### C. Ablation Studies and Visualization

In this section, we investigate the effectiveness of each component in Latte and Latte++ by thorough ablation studies and qualitative results.

TABLE IV  
CLASS-WISE PERFORMANCE (mIOU) COMPARISON ON S-TO-K.

Modality	Method	Car	Bike	Person	Road	Sidewalk	Building	Nature	Pole	O-Object	Avg
2D	xMUDA <sub>PL</sub>	52.1	14.4	1.1	62.0	30.7	44.0	54.2	19.3	<b>0.4</b>	30.9
	CoTTA	<b>57.2</b>	1.5	0.7	58.2	27.0	47.6	<b>64.8</b>	19.2	0.0	30.7
	Latte	52.9	<b>15.6</b>	<b>3.7</b>	63.0	31.3	50.1	60.9	21.9	0.3	33.3
	Latte++	53.1	15.4	<b>3.7</b>	<b>64.0</b>	<b>31.6</b>	<b>50.6</b>	61.3	<b>22.0</b>	0.3	<b>33.5</b> <sub>(+0.2)</sub>
3D	xMUDA <sub>PL</sub>	69.1	18.1	1.4	74.5	39.1	37.8	43.2	23.9	<b>1.0</b>	34.1
	CoTTA	69.2	9.1	1.2	51.2	29.5	<b>51.8</b>	<b>61.2</b>	<b>32.7</b>	0.2	35.1
	Latte	73.3	20.6	7.4	78.6	39.9	49.4	56.1	28.3	0.5	39.3
	Latte++	<b>74.3</b>	<b>20.8</b>	<b>7.5</b>	<b>80.0</b>	<b>40.7</b>	50.0	56.8	28.4	0.5	<b>39.9</b> <sub>(+0.6)</sub>
xM	xMUDA <sub>PL</sub>	70.6	26.1	1.8	75.7	38.8	39.4	46.0	27.7	<b>0.6</b>	36.3
	CoTTA	68.7	8.2	1.3	60.2	29.0	54.7	<b>64.5</b>	<b>33.7</b>	0.1	35.6
	Latte	71.8	27.2	11.1	76.9	39.0	55.8	62.0	31.0	0.2	41.7
	Latte++	<b>73.9</b>	<b>27.3</b>	<b>11.4</b>	<b>78.6</b>	<b>40.1</b>	<b>56.9</b>	62.8	31.5	0.2	<b>42.5</b> <sub>(+0.8)</sub>

1) *MM-CTTA single-modal predictions*: Besides cross-modal performance in Tab. II, single-modal predictions are also crucial metrics that reflect whether models from different modalities effectively amplify each other. To justify Latte/Latte++ can achieve better cross-modal learning compared to others, we present the sequence-wise single-modal prediction comparison with SOTA methods for both MM-CTTA benchmarks. As shown in Fig. 4, Latte prevails on most sequences in terms of either 2D (10/12 sequences) or 3D (9/12 sequences) predictions on the challenging K-to-S, while Latte+ further expands the improvement relatively by 1.1% and 1.6% on average 2D and 3D performance, respectively. On less challenging K-to-W, although the performance gap becomes narrower compared to K-to-S, a consistent sequence-wise improvement can still be observed on both Latte and



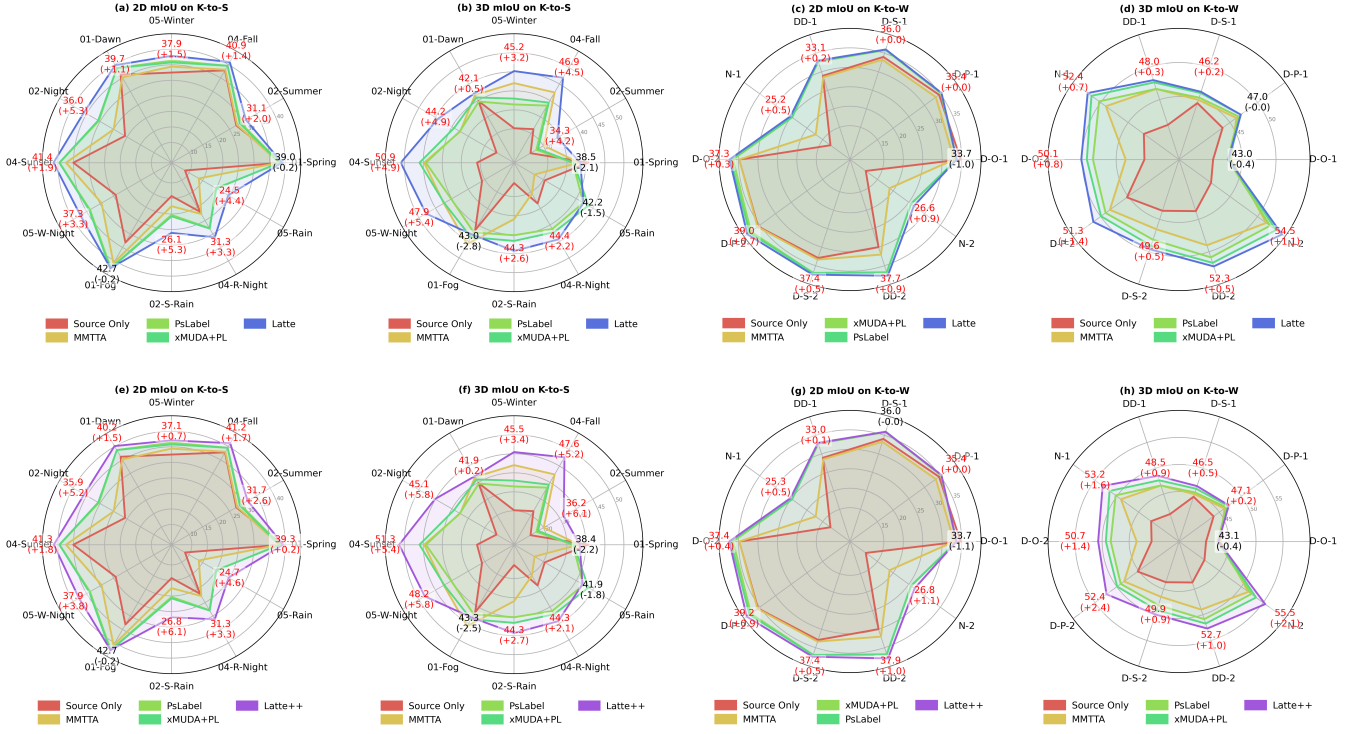


Fig. 4. Single modal predictions comparison (mIoU) on K-to-S and K-to-W. For better readability, we separately compare Latte (the upper row) and Latte++ (the bottom row) with existing SOTA MM-TTA/TTA methods. We report the performance of Latte/Latte++ for each sequence (highlighted in red if any improvement) followed by the absolute gaps compared to the previous sequence-wise highest performance in the round bracket.

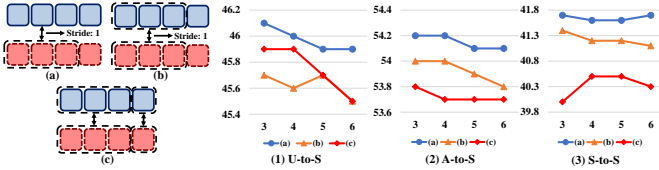


Fig. 5. Ablation studies of different frame aggregation mechanisms. Besides (a) Latte’s sliding-window aggregation, we test two different aggregation methods, including (b) replacing single frame student predictions with multiple frames in Eq. (5) and (c) adding non-overlapping aggregation to (b). Results show that our sliding-window aggregation can better evaluate the local consistency, which leads to more consistent improvement.

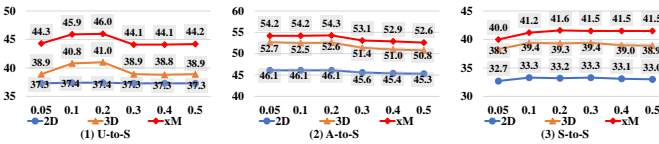


Fig. 6. Ablation studies of various ST voxel sizes.

Latte++ in either 2D or 3D performance, which justifies that Latte and Latte++ achieve better cross-modal attending compared to existing methods. Meanwhile, the sequence-wise single-modal performance of Latte++ surpasses Latte’s on most sequences (except for 2D predictions on DD-1 and N-1), exhibiting the benefit of utilizing multiple sliding windows in Latte++ compared to Latte.

## 2) MM-TTA class-wise predictions (Latte vs. Latte++):

One of our main arguments is that using various time windows for aggregation leads to better consistency evaluation

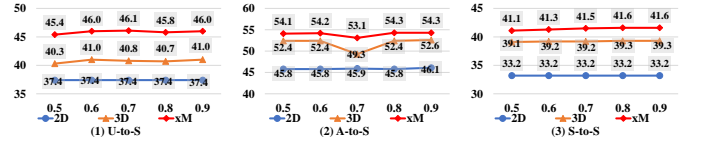


Fig. 7. Ablation studies of filtering percentile  $\alpha$  in Eq. (8).

of different semantic classes, which motivates our design of Latte++. To validate this argument, we provide the class-wise performance comparison between Latte/Latte++ and previous SOTA methods (xMUDA<sub>PL</sub> and CoTTA) on A-to-K (Tab. III) and S-to-K (Tab. IV) across all metrics. As shown in Tab. III, by utilizing multiple time windows, Latte++ improves the performance of almost all semantic classes (except for 3D predictions of “Car”) compared to Latte, resulting in an average gap of at least 0.4% on all evaluation metrics. Such consistent improvement can also be observed on S-to-K as in Tab. IV, where Latte++ achieves better or equal performance on all classes across all metrics except for 2D predictions of “Bike”, leading to an average cross-modal performance gap of 0.8%. When comparing with existing SOTA single-scan (xMUDA<sub>PL</sub>) or multi-scan (CoTTA) methods, both Latte and Latte++ achieve noticeable improvement on most classes, leading to a relative average improvement of at least 6.4% and 8.2% in terms of cross-modal predictions on both benchmarks, respectively. This universal improvement indicates the benefit of using multiple time windows for consistency evaluation.

3) *Effectiveness of cross-modal learning*: The main optimization objectives of Latte contain three parts, including ST-

TABLE V

ABLATION STUDIES ABOUT THE EFFECTIVENESS OF CROSS-MODAL LEARNING. WHEN DISABLING  $\mathbf{y}^{\text{xM}}$ , WE UTILIZE THE AVERAGE SOFTMAX OF ALL MODALITIES AS THE PSEUDO-LABELS AS A REPLACEMENT. IN EXPERIMENT NO. 8, WE REPLACE THE ST ENTROPY (ST ETY) WITH POINT-WISE ENTROPY IN EQ. (17) AND SET  $w_{\text{v}}^{\text{m}}$  IN EQ. (14) TO 0.5. HERE  $\mathcal{L}_{32}^{\text{xM}}$  AND  $\mathcal{L}_{23}^{\text{xM}}$  REFER TO THE FORMER HALF AND THE LATTER HALF IN EQ. 14, RESPECTIVELY. FOR LATTE++, † AND ‡ INDICATE USING  $\tau_d^{\text{m}}$  FOR ENTROPY AND REFERENCE PREDICTION WEIGHTING AS IN EQ. 9, RESPECTIVELY.

Method	No.	Description	$\mathbf{y}^{\text{xM}}$	$\mathcal{L}_{23}^{\text{xM}}$	$\mathcal{L}_{32}^{\text{xM}}$	$\tau_d^{\text{b}}$	$\tau_d^{\text{m} \dagger}$	$\tau_d^{\text{m} \ddagger}$	U-to-S			A-to-K			S-to-K		
									2D	3D	xM	2D	3D	xM	2D	3D	xM
-	0	Source only	-	-	-	-	-	-	31.4	41.1	43.9	47.4	17.9	44.3	23.4	36.4	38.2
Latte	1	only ST ety label	✓						36.8	34.5	43.7	43.3	42.2	49.9	22.4	30.6	33.3
	2	only ST 2D→3D		✓					32.5	34.5	41.0	41.7	42.2	48.2	27.7	30.6	32.9
	3	only ST 3D→2D			✓				36.8	39.6	42.6	43.3	50.2	48.4	22.4	26.7	25.6
	4	ST ety label + ST 2D→3D	✓	✓					<b>37.5</b>	35.8	41.0	43.6	47.5	49.8	31.0	36.0	38.4
	5	ST ety label + ST 3D→2D	✓		✓				37.4	40.9	45.9	<b>46.2</b>	52.1	53.4	32.5	38.7	39.7
	6	ST 2D↔3D		✓	✓				36.8	40.3	43.8	44.0	47.0	51.2	30.4	35.6	37.7
	7	w/o percentile in Eq. (8)	✓	✓	✓				37.4	40.3	45.4	45.7	51.4	53.2	32.9	39.0	<b>41.7</b>
	8	Point ety vs. ST ety	✓	✓	✓				37.0	40.6	45.1	45.1	51.4	52.7	31.6	36.7	38.2
	9	Latte	✓	✓	✓				37.4	<b>41.0</b>	<b>46.0</b>	46.1	<b>52.6</b>	<b>54.3</b>	<b>33.2</b>	<b>39.3</b>	41.6
Latte++	10	Disable $\tau_d^{\text{b}}$ in Eq. (10)	✓	✓	✓		✓	✓	37.5	41.0	46.3	46.2	52.8	54.8	33.2	39.6	42.1
	11	Disable $\tau_d^{\text{m}}$ for $E_{i,k}^{\text{m}}$ in Eq. (9)	✓	✓	✓	✓		✓	37.4	40.8	46.1	46.1	52.7	54.7	33.1	39.5	41.9
	12	Disable $\tau_d^{\text{m}}$ for $\bar{\mathbf{p}}_v^{\text{m}}$ in Eq. (9)	✓	✓	✓	✓	✓		37.3	40.9	46.0	46.2	52.7	54.8	33.3	39.4	41.8
	13	Disable $\tau_d^{\text{m}}$ for both in Eq. (9)	✓	✓	✓	✓	✓		37.3	40.6	45.8	46.1	52.4	54.5	32.8	39.1	41.5
	14	Latte++	✓	✓	✓	✓	✓	✓	<b>37.6</b>	<b>41.0</b>	<b>46.3</b>	<b>46.4</b>	<b>53.0</b>	<b>55.1</b>	<b>33.5</b>	<b>39.9</b>	<b>42.5</b>

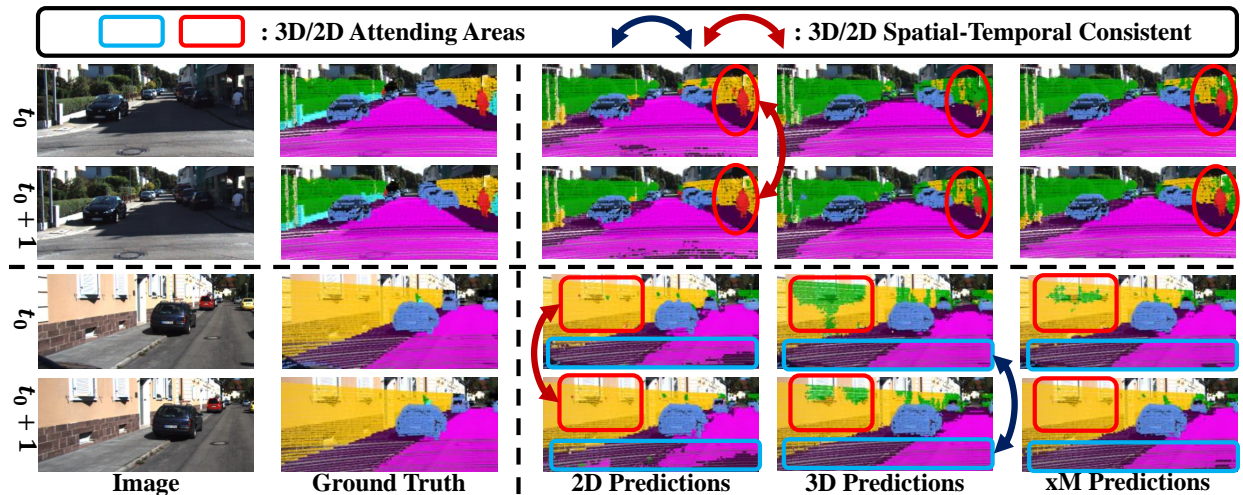


Fig. 8. Qualitative results of Latte on S-to-K. Here we visualize modality-specific predictions and cross-modal predictions from Latte during two sets of consecutive frames.

TABLE VI

PERFORMANCE (MIOU) OF LATTE++ USING DIFFERENT WINDOW SIZES.

No.	Window Sizes	U-to-S			A-to-K			S-to-K		
		2D	3D	xM	2D	3D	xM	2D	3D	xM
1	[1, 3]	<b>37.6</b>	<b>41.0</b>	46.2	<b>46.4</b>	52.9	54.9	<b>33.5</b>	39.7	42.3
2	[1, 3, 5]	<b>37.6</b>	40.9	46.2	<b>46.4</b>	52.9	54.9	<b>33.5</b>	39.8	42.4
3	[2, 3]	<b>37.6</b>	40.4	46.0	46.2	52.7	54.8	33.0	39.0	42.3
4	[3, 4]	<b>37.6</b>	<b>41.0</b>	46.1	<b>46.4</b>	52.9	55.0	33.2	39.8	42.3
5	[3]	37.4	<b>41.0</b>	46.0	46.1	52.6	54.3	33.2	39.3	41.6
6	[3, 5]	<b>37.6</b>	<b>41.0</b>	<b>46.3</b>	<b>46.4</b>	<b>53.0</b>	<b>55.1</b>	<b>33.5</b>	<b>39.9</b>	<b>42.5</b>

entropy-based cross-modal consistency (both 2D-to-3D and 3D-to-2D) and cross-entropy loss between predictions and cross-modal pseudo-labels. We justify the effectiveness by using different combinations of these components as in Tab. V. As shown from experiments No. 1 to No. 6, disabling any part of Latte causes performance decreases of more than 1.6% relatively on the cross-modal prediction (xM), which proves

the effectiveness of each component we included. A special case is No. 5 on U-to-S, where disabling ST  $\mathcal{L}_{23}^{\text{xM}}$  only leads to a minor 0.1% drop in accuracy. This is mainly because the 2D performance is already close to saturation (37.4 vs. 38.7 of Oracle TTA) without the guidance of 3D predictions. In this case, introducing 3D information to 2D is less effective compared to the other benchmarks.

Besides optimization objects, we further testify two important components of Latte, including ST-entropy-based weighting in Eq. (14) and Eq. (17) as well as percentile filtering in Eq. (8). Specifically, disabling percentile filtering as in No. 7 leads to a relative accuracy drop of more than 0.5% across all benchmarks while utilizing point-wise entropy instead of our ST entropy as in No. 8 relatively degenerates the performance by 2.0%, which justifies that ST entropy better estimates the prediction reliability compared to the point-wise entropy.

In terms of Latte++, we mainly validate the effectiveness of two components, including the initial weight  $\tau_d^{\text{b}}$  (Eq. 10)

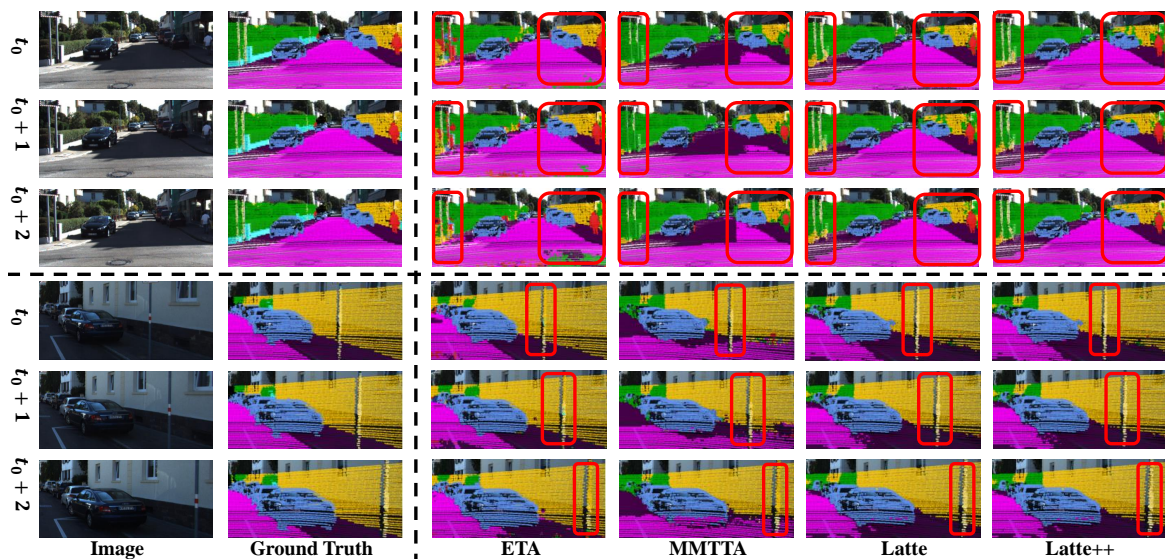


Fig. 9. Qualitative comparison with ETA [36] and MMTTA [44] on S-to-K. Red boxes highlight the area where Latte produces more accurate predictions compared to ETA and MMTTA. Figure best viewed in color and zoomed in.

and multi-window weight  $\tau_d^m$  (Eq. 9). Specifically, we disable any of these adaptive weights by replacing them with 0.5. As shown in No. 10-12, disabling either  $\tau_d^b$  or  $\tau_d^m$  leads to a noticeable drop in both single-modal and cross-modal prediction accuracy, while those Latte++ variants can still surpass vanilla Latte consistently in most cases. However, when disabling  $\tau_d^m$  for both ST entropy and reference prediction in Eq. 9 in No. 13, Latte++ achieves inferior performance compared to Latte, which justifies the effectiveness of assigning adaptive weights based on ST entropy of different time windows.

4) *Different frame aggregation mechanisms*: One of the core designs of Latte is the sliding-window frame aggregation, which is designed to capture temporally local correspondences and estimate their prediction consistency. To justify the aforementioned claim, we compare our sliding-window aggregation with two aggregation variants as shown in Fig. 5. Specifically, variant (b) regards all student prediction frames rather than a single frame within the time window as the query in Eq. (5), while variant (c) further utilizes a non-overlapping sliding strategy. According to Fig. 5, our sliding-window aggregation surpasses the other two aggregation variants under all sizes of time windows across three benchmarks, which justifies the effectiveness of our method. The inferior performance of variants (b) and (c) could be due to two factors. Firstly, aggregating student predictions could be an inferior option since student predictions tend to be less stable, and aggregating multiple frames can therefore lead to noisy queries for cross-modal learning. Secondly, non-overlapping aggregation can result in a miss-checking area on the boundary of each time window, which leads to unrepresentative entropy estimation for some ST voxels. Another observation is that utilizing a smaller sliding window can usually yield better performance since temporally local consistency can be captured. This justifies the effectiveness of estimating prediction reliability through temporally local consistency.

For Latte++, we testify the performance of Latte++ when

utilizing different combinations of window sizes as shown in Tab. VI. Among all alternatives, the combination of [3, 5] achieves SOTA performance among all evaluation metrics, and introducing a window size of 1 brings a trivial difference (No. 6 vs. No. 2). Note that compared to vanilla Latte which utilizes a single pre-defined time window for consistency check, Latte++ with an arbitrary combination of different windows (No. 1-4, and No. 6) brings non-trivial and consistent improvement across three MM-TTA benchmarks. Especially on more challenging A-to-K and S-to-K, the relative gap on cross-modal predictions between Latte++ with arbitrary time window combinations and vanilla Latte consistently exceeds 1.0%, which validates the effectiveness of aggregating ST entropy under different time windows.

5) *Parameter sensitivity analysis*.: To testify whether Latte is sensitive towards hyper-parameter settings, we conduct sensitivity analysis on Latte across three benchmarks. Here we illustrate the sensitivity analysis of two hyper-parameters of Latte, including ST voxel size and filtering percentile  $\alpha$  as shown in Fig. 6 and Fig. 7, respectively. In terms of ST voxel sizes, one can tell from Fig. 6 that all benchmarks share the same optimal voxel size as 0.2, where performance drops as the voxel size becomes too large or too small. This is mainly because large voxels could cause boundary ambiguity while small voxels contain insufficient representative points for evaluation. As for filtering percentile  $\alpha$ , non-trivial improvement can be observed on U-to-S and A-to-K when  $\alpha \geq 0.8$ , while a lower  $\alpha$  begins to discard more confident ST voxels leading to a slight drop in accuracy. On S-to-K, Latte without filtering (*i.e.*, No. 7 in Tab. V) performs slightly better on cross-modal predictions with a minor gap of 0.1%, while it can also be observed that setting  $\alpha$  as 0.9 leads to an improvement of 0.3% on both modality-specific predictions, which justifies the overall effectiveness of our filtering procedures.

6) *Qualitative results*: Our main motivation is utilizing prediction consistency of spatial-temporal correspondences to



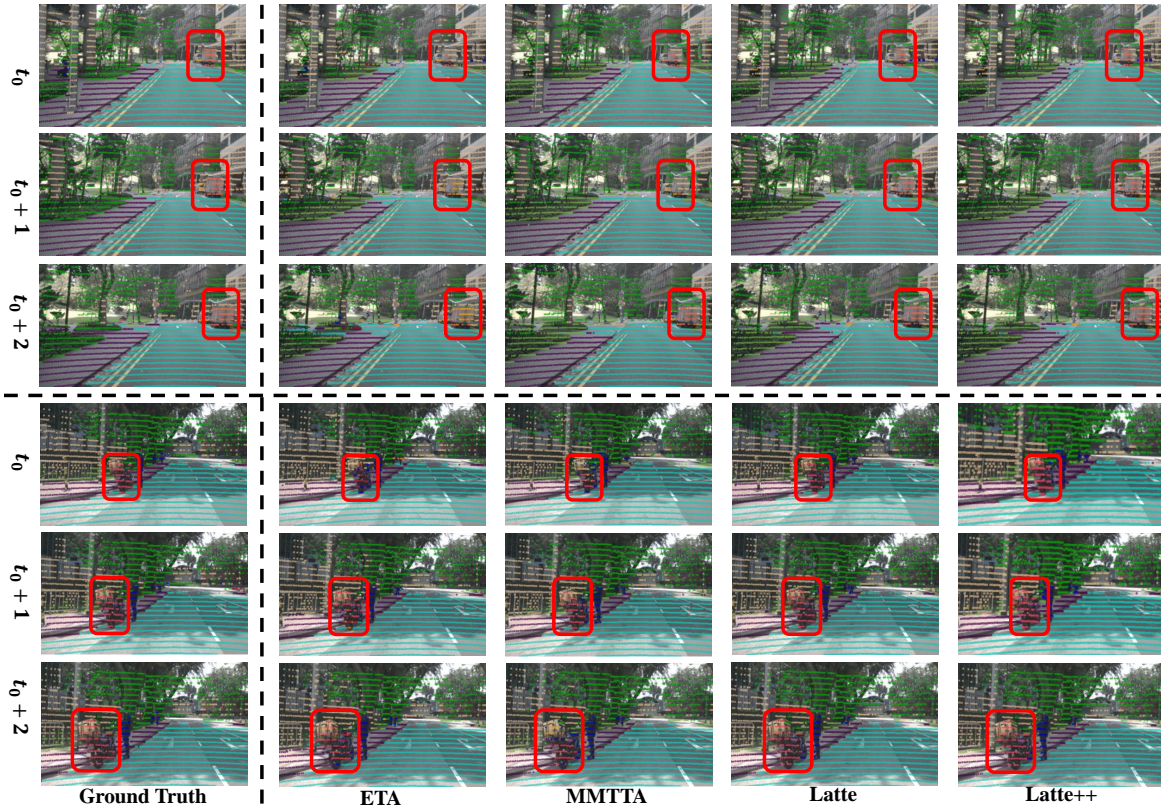


Fig. 10. Qualitative comparison with ETA [36] and MMTA [44] on U-to-S. Red boxes highlight the area where Latte produces more accurate predictions compared to ETA and MMTA. Figure best viewed in color and zoomed in.

estimate modality reliability and achieve better cross-modal attending. As shown in Fig. 8, both Latte and Latte++ can effectively attend the modality with more consistent predictions in spatial-temporal correspondences and therefore improve the cross-modal prediction consistency across time. For instance, Latte and Latte++ successfully attend to the stable 2D predictions pedestrian in the upper set of consecutive frames, suppressing the spatial-temporal inconsistency from 3D predictions. Similar observations can also be found in the lower sample, where the more consistent 2D predictions of buildings in the red rectangle and 3D predictions of roads in the blue rectangle prevail.

To demonstrate the improvement brought by Latte, we provide some additional qualitative comparison between Latte/Latte++ and previous SOTA TTA (ETA [36]) and MM-TTA (MMTTA [44]) methods on U-to-S and S-to-K. As shown in Fig. 9 and Fig. 10, the cross-modal predictions from Latte and Latte++ are more accurate compared to ETA and MMTA (*e.g.*, more accurate pole recognition on the lower set of consecutive frames in Fig. 9). Furthermore, the predictions from Latte and Latte++ are more consistent across time. For instance, the pedestrians and poles in the red rectangles in Fig. 9 as well as the motorcycle and the truck in Fig. 10 can be consistently recognized by Latte/Latte++, while both ETA and MMTA suffer from the instability of single-frame predictions. This justifies the effectiveness of Latte and Latte++ and the improvement brought by our multi-frame aggregation strategy.

## V. CONCLUSION

In this paper, we propose a novel MM-TTA method called Latte, which leverages prediction consistency of spatial-temporal correspondences in MM-TTA for 3D segmentation. Latte utilizes a sliding-window frame aggregation to extract ST voxels and estimates temporally local consistency by the ST entropy of each modality. By attending to the modality with more consistency, Latte can achieve stable improvement on challenging MM-TTA scenarios. We further extend Latte to Latte++, leveraging multiple time windows for a more accurate estimation of voxel-wise prediction reliability. Despite its effectiveness, both Latte and Latte++ struggle to rectify consistently wrong predictions across time, which is challenging and worth further investigation in the future.

## REFERENCES

- [1] Awais, M., Naseer, M., Khan, S., Anwer, R.M., Cholakkal, H., Shah, M., Yang, M.H., Khan, F.S.: Foundation models defining a new era in vision: a survey and outlook. *IEEE Transactions on Pattern Analysis and Machine Intelligence* (2025)
- [2] Behley, J., Garbade, M., Milioto, A., Quenzel, J., Behnke, S., Stachniss, C., Gall, J.: Semantickitti: A dataset for semantic scene understanding of lidar sequences. In: *Proceedings of the IEEE/CVF International Conference on Computer Vision*. pp. 9297–9307 (2019)
- [3] Boudiaf, M., Mueller, R., Ben Ayed, I., Bertinetto, L.: Parameter-free online test-time adaptation. In: *Proceedings of the IEEE/CVF Conference on Computer Vision and Pattern Recognition*. pp. 8344–8353 (2022)

- [4] Caesar, H., Bankiti, V., Lang, A.H., Vora, S., Liong, V.E., Xu, Q., Krishnan, A., Pan, Y., Baldan, G., Beijbom, O.: nusences: A multimodal dataset for autonomous driving. In: Proceedings of the IEEE/CVF Conference on Computer Vision and Pattern Recognition. pp. 11621–11631 (2020)
- [5] Cao, H., Xu, Y., Yang, J., Yin, P., Ji, X., Yuan, S., Xie, L.: Reliable spatial-temporal voxels for multi-modal test-time adaptation. In: European Conference on Computer Vision. pp. 232–249. Springer (2025)
- [6] Cao, H., Xu, Y., Yang, J., Yin, P., Yuan, S., Xie, L.: Mopa: Multi-modal prior aided domain adaptation for 3d semantic segmentation. arXiv preprint arXiv:2309.11839 (2023)
- [7] Cao, H., Xu, Y., Yang, J., Yin, P., Yuan, S., Xie, L.: Multi-modal continual test-time adaptation for 3d semantic segmentation. In: Proceedings of the IEEE/CVF International Conference on Computer Vision (ICCV). pp. 18809–18819 (October 2023)
- [8] Chen, D., Wang, D., Darrell, T., Ebrahimi, S.: Contrastive test-time adaptation. In: Proceedings of the IEEE/CVF Conference on Computer Vision and Pattern Recognition. pp. 295–305 (2022)
- [9] Chen, R., Liu, Y., Kong, L., Zhu, X., Ma, Y., Li, Y., Hou, Y., Qiao, Y., Wang, W.: Clip2scene: Towards label-efficient 3d scene understanding by clip. In: Proceedings of the IEEE/CVF Conference on Computer Vision and Pattern Recognition. pp. 7020–7030 (2023)
- [10] Chen, X., Milioto, A., Palazzolo, E., Giguere, P., Behley, J., Stachniss, C.: Suma++: Efficient lidar-based semantic slam. In: 2019 IEEE/RSJ International Conference on Intelligent Robots and Systems (IROS). pp. 4530–4537. IEEE (2019)
- [11] Choy, C., Gwak, J., Savarese, S.: 4d spatio-temporal convnets: Minkowski convolutional neural networks. In: Proceedings of the IEEE/CVF Conference on Computer Vision and Pattern Recognition. pp. 3075–3084 (2019)
- [12] Deng, T., Shen, G., Qin, T., Wang, J., Zhao, W., Wang, J., Wang, D., Chen, W.: Ploglam: Progressive neural scene representation with local to global bundle adjustment. In: Proceedings of the IEEE/CVF Conference on Computer Vision and Pattern Recognition. pp. 19657–19666 (2024)
- [13] Ding, R., Yang, J., Xue, C., Zhang, W., Bai, S., Qi, X.: Lowis3d: Language-driven open-world instance-level 3d scene understanding. IEEE Transactions on Pattern Analysis and Machine Intelligence (2024)
- [14] Fan, H., Yang, Y., Kankanhalli, M.: Point 4d transformer networks for spatio-temporal modeling in point cloud videos. In: Proceedings of the IEEE/CVF Conference on Computer Vision and Pattern Recognition. pp. 14204–14213 (2021)
- [15] Fan, H., Yu, X., Ding, Y., Yang, Y., Kankanhalli, M.: Pstnet: Point spatio-temporal convolution on point cloud sequences. arXiv preprint arXiv:2205.13713 (2022)
- [16] Feng, D., Haase-Schütz, C., Rosenbaum, L., Hertlein, H., Glaeser, C., Timm, F., Wiesbeck, W., Dietmayer, K.: Deep multi-modal object detection and semantic segmentation for autonomous driving: Datasets, methods, and challenges. IEEE Transactions on Intelligent Transportation Systems **22**(3), 1341–1360 (2020)
- [17] Geyer, J., Kassahun, Y., Mahmudi, M., Ricou, X., Durgesh, R., Chung, A.S., Hauswald, L., Pham, V.H., Mühlegg, M., Dorn, S., et al.: A2d2: Audi autonomous driving dataset. arXiv preprint arXiv:2004.06320 (2020)
- [18] Gong, T., Jeong, J., Kim, T., Kim, Y., Shin, J., Lee, S.J.: Note: Robust continual test-time adaptation against temporal correlation. Advances in Neural Information Processing Systems **35**, 27253–27266 (2022)
- [19] Gong, T., Jeong, J., Kim, T., Kim, Y., Shin, J., Lee, S.J.: Robust continual test-time adaptation: Instance-aware bn and prediction-balanced memory. arXiv preprint arXiv:2208.05117 (2022)
- [20] Goyal, S., Sun, M., Raghunathan, A., Kolter, J.Z.: Test time adaptation via conjugate pseudo-labels. In: Advances in Neural Information Processing Systems (2022)
- [21] Graham, B.: Sparse 3d convolutional neural networks. arXiv preprint arXiv:1505.02890 (2015)
- [22] Guo, Y., Wang, H., Hu, Q., Liu, H., Liu, L., Bennamoun, M.: Deep learning for 3d point clouds: A survey. IEEE Transactions on Pattern Analysis and Machine Intelligence **43**(12), 4338–4364 (2020)
- [23] Hong, F., Kong, L., Zhou, H., Zhu, X., Li, H., Liu, Z.: Unified 3d and 4d panoptic segmentation via dynamic shifting networks. IEEE Transactions on Pattern Analysis and Machine Intelligence (2024)
- [24] Huang, S., Gojcic, Z., Huang, J., Wieser, A., Schindler, K.: Dynamic 3d scene analysis by point cloud accumulation. In: European Conference on Computer Vision. pp. 674–690. Springer (2022)
- [25] Jaritz, M., Vu, T.H., De Charette, R., Wirbel, É., Pérez, P.: Cross-modal learning for domain adaptation in 3d semantic segmentation. IEEE Transactions on Pattern Analysis and Machine Intelligence **45**(2), 1533–1544 (2022)
- [26] Ji, X., Yuan, S., Yin, P., Xie, L.: Lio-gvm: an accurate, tightly-coupled lidar-inertial odometry with gaussian voxel map. IEEE Robotics and Automation Letters (2024)
- [27] Kirillov, A., Mintun, E., Ravi, N., Mao, H., Rolland, C., Gustafson, L., Xiao, T., Whitehead, S., Berg, A.C., Lo, W.Y., et al.: Segment anything. In: Proceedings of the IEEE/CVF International Conference on Computer Vision. pp. 4015–4026 (2023)
- [28] Kundu, J.N., Venkat, N., Babu, R.V., et al.: Universal source-free domain adaptation. In: Proceedings of the IEEE/CVF conference on computer vision and pattern recognition. pp. 4544–4553 (2020)
- [29] Li, M., Zhang, Y., Xie, Y., Gao, Z., Li, C., Zhang, Z., Qu, Y.: Cross-domain and cross-modal knowledge distillation in domain adaptation for 3d semantic segmentation. In: Proceedings of the 30th ACM International Conference on Multimedia. pp. 3829–3837 (2022)
- [30] Liang, J., He, R., Tan, T.: A comprehensive survey on test-time adaptation under distribution shifts. International Journal of Computer Vision pp. 1–34 (2024)
- [31] Liang, J., Hu, D., Feng, J.: Do we really need to access the source data? source hypothesis transfer for unsupervised domain adaptation. In: International Conference on Machine Learning. pp. 6028–6039. PMLR (2020)
- [32] Liang, J., Hu, D., Wang, Y., He, R., Feng, J.: Source data-absent unsupervised domain adaptation through hypothesis transfer and labeling transfer. IEEE Transactions on Pattern Analysis and Machine Intelligence **44**(11), 8602–8617 (2021)
- [33] Liu, W., Luo, Z., Cai, Y., Yu, Y., Ke, Y., Junior, J.M., Gonçalves, W.N., Li, J.: Adversarial unsupervised domain adaptation for 3d semantic segmentation with multi-modal learning. ISPRS Journal of Photogrammetry and Remote Sensing **176**, 211–221 (2021)
- [34] Liu, Y., Kothari, P., Van Delft, B., Bellot-Gurlet, B., Mordan, T., Alahi, A.: Ttt++: When does self-supervised test-time training fail or thrive? Advances in Neural Information Processing Systems **34**, 21808–21820 (2021)
- [35] Niu, S., Miao, C., Chen, G., Wu, P., Zhao, P.: Test-time model adaptation with only forward passes. In: The International Conference on Machine Learning (2024)
- [36] Niu, S., Wu, J., Zhang, Y., Chen, Y., Zheng, S., Zhao, P., Tan, M.: Efficient test-time model adaptation without forgetting. In: International Conference on Machine Learning. pp. 16888–16905. PMLR (2022)
- [37] Niu, S., Wu, J., Zhang, Y., Wen, Z., Chen, Y., Zhao, P., Tan, M.: Towards stable test-time adaptation in dynamic wild world. arXiv preprint arXiv:2302.12400 (2023)
- [38] Peng, D., Lei, Y., Li, W., Zhang, P., Guo, Y.: Sparse-to-dense feature matching: Intra and inter domain cross-modal learning in domain adaptation for 3d semantic segmentation. In: Proceedings of the IEEE/CVF International Conference on Computer Vision. pp. 7108–7117 (2021)
- [39] Peng, X., Chen, R., Qiao, F., Kong, L., Liu, Y., Sun, Y., Wang, T., Zhu, X., Ma, Y.: Learning to adapt sam for segmenting cross-domain point clouds. In: European Conference on Computer Vision. pp. 54–71. Springer (2025)
- [40] Piergiovanni, A., Casser, V., Ryoo, M.S., Angelova, A.: 4d-net for learned multi-modal alignment. In: Proceedings of the IEEE/CVF International Conference on Computer Vision. pp. 15435–15445 (2021)
- [41] Qi, C.R., Su, H., Mo, K., Guibas, L.J.: Pointnet: Deep learning on point sets for 3d classification and segmentation. In: Proceedings of the IEEE Conference on Computer Vision and Pattern Recognition. pp. 652–660 (2017)
- [42] Radford, A., Kim, J.W., Hallacy, C., Ramesh, A., Goh, G., Agarwal, S., Sastry, G., Askell, A., Mishkin, P., Clark, J., et al.: Learning transferable visual models from natural language supervision. In: International Conference on Machine Learning. pp. 8748–8763. PMLR (2021)
- [43] Saltori, C., Krivosheev, E., Lathuilière, S., Sebe, N., Galasso, F., Fiameni, G., Ricci, E., Poiesi, F.: Gippo: Geometrically informed propagation for online adaptation in 3d lidar segmentation. In: European Conference on Computer Vision. pp. 567–585. Springer (2022)
- [44] Shin, I., Tsai, Y.H., Zhuang, B., Schuler, S., Liu, B., Garg, S., Kweon, I.S., Yoon, K.J.: Mm-tta: multi-modal test-time adaptation for 3d semantic segmentation. In: Proceedings of the IEEE/CVF Conference on Computer Vision and Pattern Recognition. pp. 16928–16937 (2022)
- [45] Simons, C., Raychaudhuri, D.S., Ahmed, S.M., You, S., Karydis, K., Roy-Chowdhury, A.K.: Summit: Source-free adaptation of uni-modal models to multi-modal targets. In: Proceedings of the IEEE/CVF International Conference on Computer Vision (ICCV). pp. 1239–1249 (October 2023)
- [46] Song, J., Lee, J., Kweon, I.S., Choi, S.: Ecotta: Memory-efficient continual test-time adaptation via self-distilled regularization. In: Pro-



- ceedings of the IEEE/CVF Conference on Computer Vision and Pattern Recognition. pp. 11920–11929 (2023)
- [47] Su, Y., Xu, X., Li, T., Jia, K.: Revisiting realistic test-time training: Sequential inference and adaptation by anchored clustering regularized self-training. arXiv preprint arXiv:2303.10856 (2023)
- [48] Tang, H., Liu, Z., Zhao, S., Lin, Y., Lin, J., Wang, H., Han, S.: Searching efficient 3d architectures with sparse point-voxel convolution. In: European Conference on Computer Vision. pp. 685–702. Springer (2020)
- [49] Tarvainen, A., Valpola, H.: Mean teachers are better role models: Weight-averaged consistency targets improve semi-supervised deep learning results. *Advances in Neural Information Processing Systems* **30** (2017)
- [50] Vedula, S., Baker, S., Rander, P., Collins, R., Kanade, T.: Three-dimensional scene flow. In: Proceedings of the Seventh IEEE International Conference on Computer Vision. vol. 2, pp. 722–729. IEEE (1999)
- [51] Vizzo, I., Guadagnino, T., Mersch, B., Wiesmann, L., Behley, J., Stachniss, C.: Kiss-icp: In defense of point-to-point icp—simple, accurate, and robust registration if done the right way. *IEEE Robotics and Automation Letters* **8**(2), 1029–1036 (2023)
- [52] Vogel, C., Schindler, K., Roth, S.: 3d scene flow estimation with a rigid motion prior. In: 2011 International Conference on Computer Vision. pp. 1291–1298. IEEE (2011)
- [53] Vogel, C., Schindler, K., Roth, S.: Piecewise rigid scene flow. In: Proceedings of the IEEE International Conference on Computer Vision. pp. 1377–1384 (2013)
- [54] Wang, D., Shelhamer, E., Liu, S., Olshausen, B., Darrell, T.: Tent: Fully test-time adaptation by entropy minimization. In: International Conference on Learning Representations (2021), <https://openreview.net/forum?id=uX13bZLkr3c>
- [55] Wang, J.K., Wibisono, A.: Towards understanding gd with hard and conjugate pseudo-labels for test-time adaptation. arXiv preprint arXiv:2210.10019 (2022)
- [56] Wang, Q., Fink, O., Van Gool, L., Dai, D.: Continual test-time domain adaptation. In: Proceedings of the IEEE/CVF Conference on Computer Vision and Pattern Recognition. pp. 7201–7211 (2022)
- [57] Wu, Y., Xing, M., Zhang, Y., Luo, X., Xie, Y., Qu, Y.: Unidseg: Unified cross-domain 3d semantic segmentation via visual foundation models prior. In: The Thirty-eighth Annual Conference on Neural Information Processing Systems (2024)
- [58] Wu, Y., Xing, M., Zhang, Y., Xie, Y., Qu, Y.: Clip2uda: Making frozen clip reward unsupervised domain adaptation in 3d semantic segmentation. In: Proceedings of the 32nd ACM International Conference on Multimedia. pp. 8662–8671 (2024)
- [59] Wyner, A.: Recent results in the shannon theory. *IEEE Transactions on information Theory* **20**(1), 2–10 (1974)
- [60] Xie, E., Wang, W., Yu, Z., Anandkumar, A., Alvarez, J.M., Luo, P.: Segformer: Simple and efficient design for semantic segmentation with transformers. *Advances in Neural Information Processing Systems* **34**, 12077–12090 (2021)
- [61] Xing, B., Ying, X., Wang, R., Yang, J., Chen, T.: Cross-modal contrastive learning for domain adaptation in 3d semantic segmentation. In: Proceedings of the AAAI Conference on Artificial Intelligence. vol. 37, pp. 2974–2982 (2023)
- [62] Xu, J., Miao, Z., Zhang, D., Pan, H., Liu, K., Hao, P., Zhu, J., Sun, Z., Li, H., Zhan, X.: Int: Towards infinite-frames 3d detection with an efficient framework. In: European Conference on Computer Vision. pp. 193–209. Springer (2022)
- [63] Yin, P., Cao, H., Nguyen, T.M., Yuan, S., Zhang, S., Liu, K., Xie, L.: Outram: One-shot global localization via triangulated scene graph and global outlier pruning. arXiv preprint arXiv:2309.08914 (2023)
- [64] Yuan, L., Xie, B., Li, S.: Robust test-time adaptation in dynamic scenarios. In: Proceedings of the IEEE/CVF Conference on Computer Vision and Pattern Recognition. pp. 15922–15932 (2023)
- [65] Zhang, M., Levine, S., Finn, C.: Memo: Test time robustness via adaptation and augmentation. *Advances in Neural Information Processing Systems* **35**, 38629–38642 (2022)
- [66] Zhao, B., Chen, C., Xia, S.T.: DELTA: DEGRADATION-FREE FULLY TEST-TIME ADAPTATION. In: The Eleventh International Conference on Learning Representations (2023), <https://openreview.net/forum?id=eGm22rqG93>
- [67] Zheng, X., Zhou, P.Y., Vasilakos, A.V., Wang, L.: 360sfuda++: Towards source-free uda for panoramic segmentation by learning reliable category prototypes. *IEEE Transactions on Pattern Analysis and Machine Intelligence* (2024)

## VI. BIOGRAPHY SECTION



transfer learning and multi-modal learning.

**Haozhi Cao** received the B.Eng. from the School of Electrical Engineering and Automation, Wuhan University in 2019, and the M.Eng. degree from the School of Electrical and Electronic Engineering, Nanyang Technological University (NTU), Singapore in 2021. He is currently a Ph.D. student in the School of Electrical and Electronic Engineering, NTU. He is also working as a Research Associate at the Centre for Advanced Robotics Technology (CARTIN), NTU. His research interests include deep learning with applications in video understanding,

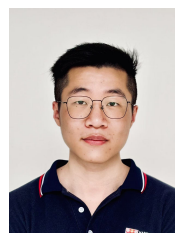


and transfer learning. His research also touches on human pose estimation via radio frequency vision. He was the co-organizer of the UG2+ Challenge for Computational Photography and Visual Recognition, held in conjunction with CVPR 2021, 2022, and 2024.

**Yuecong Xu** is an Educator Track Lecturer at the Department of Electrical and Computer Engineering, National University of Singapore. He received a B.Eng. from the School of Electrical and Electronic Engineering, Nanyang Technological University, Singapore in 2017, and a Ph.D. degree from Nanyang Technological University (NTU), Singapore in 2021. He was the receiver of the Nanyang President's Graduate Scholarship. His research focuses on robust and secure video and 3D data understanding and analysis based on deep learning



**Pengyu Yin** received the B.Eng. and M.Eng. degrees from the College of Artificial Intelligence, Xi'an Jiaotong University in 2018 and 2021 respectively. And a double degree in engineering (Diplôme d'Ingénieur) from CentraleSupélec (Gif-sur-Yvette) in 2021. He is currently a Ph.D. student in the School of Electrical and Electronic Engineering, NTU. His research interests include point cloud registration and general pose estimation problems.



**Xingyu Ji** received the B.Eng. from the School of Optoelectronic Science and Engineering, University of Electronic Science and Technology of China in 2020, and the M.Sc. degree from the School of Electrical and Electronic Engineering, Nanyang Technological University (NTU). He is currently a Ph.D. student in the School of Electrical and Electronic Engineering, NTU. His research interests include LiDAR-based localization and mapping.



**Shenghai Yuan** received his B.S. and Ph.D. degrees in Electrical and Electronic Engineering from Nanyang Technological University, Singapore, in 2013 and 2019, respectively. He specializes in robotics perception and navigation and is currently a postdoctoral senior research fellow at the Centre for Advanced Robotics Technology Innovation (CARTIN) at Nanyang Technological University.

Dr. Yuan has made significant contributions to the field, with over 60 published papers in renowned journals such as TRO, IJRR, TIE, and RAL, and at prestigious conferences including ICRA, CVPR, ICCV, NeurIPS, and IROS. His editorial roles include serving as an associate editor for the Unmanned Systems Journal and as a guest editor for the Electronics Special Issue on Advanced Technologies of Navigation for Intelligent Vehicles.

His work has earned him numerous accolades, including second place in the academic track of the 2021 Hilti SLAM Challenge, third place in the visual-inertial track of the 2023 ICCV SLAM Challenge, and the Best Entertainment and Amusement Paper Award at IROS 2023. In addition, Dr. Yuan organized the CARIC UAV Swarm Challenge and Workshop at the 2023 CDC, the UG2 Anti-drone Challenge and Workshop at CVPR 2024, and the second CARIC UAV Swarm Challenge and Workshop at IROS 2024.



**Jianfei Yang** is currently an assistant professor at the School of Mechanical and Aerospace Engineering and the School of Electrical and Electronics Engineering at Nanyang Technological University (NTU), Singapore. He received his B.Eng. from Sun Yat-sen University in 2016 and his Ph.D. from NTU in 2020. Following his Ph.D., he worked as a senior research engineer at BEARS, University of California, Berkeley. He then worked as a presidential postdoc at NTU from 2021 to 2023. In 2024, he was a visiting scholar at the University of Tokyo and

Harvard University. His research interests include physical AI, deep learning, multimodal learning, and artificial intelligence of things. He has received the best Ph.D. thesis award from NTU and has won several international AI challenges in computer vision and interdisciplinary research fields.



**Lihua Xie** received the Ph.D. degree in electrical engineering from the University of Newcastle, Australia, in 1992. Since 1992, he has been with the School of Electrical and Electronic Engineering, Nanyang Technological University, Singapore, where he is currently President's Chair in control engineering and Director, Center for Advanced Robotics Technology Innovation. He has served as the Head of Division of Control and Instrumentation and Co-Director, Delta-NTU Corporate Lab for Cyber-Physical Systems. He held teaching appointments in the Department of Automatic Control, Nanjing University of Science and Technology from 1986 to 1989.

Dr Xie's research interests include robust control and estimation, networked control systems, multi-agent networks, and unmanned systems. He has published 10 books and numerous papers in the areas, and holds 25 patents/technical disclosures. He was listed as a highly cited researcher by Thomson Reuters and Clarivate Analytics. He is an Editor-in-Chief for Unmanned Systems and has served as Editor for IET Book Series in Control and Associate Editor for a number of journals including IEEE Transactions on Automatic Control, Automatica, IEEE Transactions on Control Systems Technology, IEEE Transactions on Network Control Systems, etc. He was an IEEE Distinguished Lecturer (Jan 2012 – Dec 2014) and the General Chair of the 62nd IEEE Conference on Decision and Control (CDC 2023). He is currently Vice-President of IEEE Control System Society. Dr Xie is Fellow of Academy of Engineering Singapore, IEEE, IFAC, and CAA.

Dr Xie's research interests include robust control and estimation, networked control systems, multi-agent networks, and unmanned systems. He has published 10 books and numerous papers in the areas, and holds 25 patents/technical disclosures. He was listed as a highly cited researcher by Thomson Routers and Clarivate Analytics. He is an Editor-in-Chief for Unmanned Systems and has served as Editor for IET Book Series in Control and Associate Editor for a number of journals including IEEE Transactions on Automatic Control, Automatica, IEEE Transactions on Control Systems Technology, IEEE Transactions on Network Control Systems, etc. He was an IEEE Distinguished Lecturer (Jan 2012 – Dec 2014) and the General Chair of the 62nd IEEE Conference on Decision and Control (CDC 2023). He is currently Vice-President of IEEE Control System Society. Dr Xie is Fellow of Academy of Engineering Singapore, IEEE, IFAC, and CAA.